Diploma thesis

The Role of A-971432, a Selective Agonist of Sphingosine 1-Phosphate Receptor 5, in the Experimental Model of Nephrotoxic Serum Nephritis

submitted by

Nicole Patrizia Bättig

to attain the academic degree

Doktor(in) der gesamten Heilkunde

(Dr. med. univ.)

at the

Medical University of Graz

conducted at the

Department of Internal Medicine

Clinical Division of Nephrology

under supervision of

Assoz. Prof.in Priv.-Doz.in Dr.in med.univ. Kathrin Eller

and

Dr.in med.univ. Katharina Artinger, PhD

Graz, July 29, 2022

Affidavit

I declare that I have written the submitted thesis independently and without any illegitimate assistance from third parties. Furthermore, I confirm to not have used any other than the declared sources for the preparation of this academic work. All used sources have been indicated as such and acknowledged by means of complete references in the text.

Graz, July 29, 2022 *Nicole Patrizia Bättig e.h.*

Danksagungen

Für die hervorragende Begleitung dieser Diplomarbeit möchte ich meinen beiden Betreuerinnen Kathrin Eller und Katharina Artinger danken. Dank ihrer herausragenden Expertise konnten sie mir immer wieder in meiner Recherche wertvolle Hinweise geben und meine Fragen ausführlich beantworten. Ein besonderer Dank geht an Corinna Schabhüttl, die mich stets geduldig in die verschiedenen Labormethoden einführte und mir mit ihrer fröhlichen Art jederzeit mit Rat und Tat zur Seite stand. Vielen Dank an alle Mitarbeiter des nephrologischen Labors für die herzliche Aufnahme ins Team und die tatkräftige Unterstützung und interessanten Diskussionen während der Laborarbeit.

Ein Dank, welcher schwer in Worte zu fassen ist, geht an meine Eltern, welche mir das Studium der Humanmedizin ermöglicht haben. Danke für eure tatkräftige und bedingungslose Unterstützung in jeder Lebenslage.

Danke an meine beiden Schwestern Corinne und Sandra und an meine langjährige beste Freundin Taja für die stets offenen Ohren und aufmunternden Worte.

Nicht zuletzt auch danke an meinen Freund Alexander für die inspirierenden Gespräche und die Unterstützung zur jeder Tag- und Nachtzeit.

List of contents

Glossary and abbreviations

ABC ..... *Avidin-biotin complex*
AEC *3-amino-9-ethylcarbazole*
ANA ..... *Anti-nuclear antibody*
ANCA ..... *Antineutrophil cytoplasmic autoantibodies*
ATP ..... *Adenosine triphosphate*
BLyS ..... *B-lymphocyte stimulator*
BSA ..... *Bovine serum albumin*
CA ..... *California*
CD ..... *Cluster of differentiation*
CGN ..... *Crescentic glomerulonephritis*
CKD ..... *Chronic kidney disease*
CKD-EPI ..... *Chronic Kidney Disease Epidemiology Collaboration*
CLSM ..... *Confocal laser scanning microscopy*
CNS ..... *Central nervous systems*
CTGF ..... *Connective tissue growth factor*
DC ..... *Dendritic cell*
ECPR ..... *Endothelial protein C receptor*
eGFR ..... *Estimated glomerular filtration rate*
EGPA ..... *Eosinophilic granulomatosis with polyangiitis*
ELISA ..... *Enzyme-linked immunosorbent assay*
EU ..... *European Union*
Foxp3 ..... *Forkhead box P3*
GBM ..... *Glomerular basement membrane*
GFR ..... *Glomerular filtration rate*
GN ..... *Glomerulonephritis*
GPA ..... *Granulomatosis with polyangiitis*
GPI ..... *Glycosylphosphatidylinositol*
HLA ..... *Human leukocyte antigen*
HPF ..... *High power field*
HRP ..... *Horseradish peroxidase*
Ig ..... *Immunoglobulin*
IL ..... *Interleukin*, *Illinois*
INF-γ ..... *Interferon-γ*
iNKT cell ..... *Invariant natural killer T cell*
KDIGO ..... *Kidney Disease: Improving Global Outcomes*
LAMP ..... *Lysosome-associated membrane glycoprotein*
LPF ..... *Low power field*
MC ..... *Mesangial cell*
MHC ..... *Major histocompatibility complex*
MI ..... *Michigan*
MMF ..... *Mycophenolate mofetil*
MO ..... *Missouri*
MPA ..... *Microscopic polyangiitis*
MPGN ..... *Membranoproliferative glomerulonephritis*
MPO ..... *Myeloperoxidase*
mRNA ..... *Messenger ribonucleic acid*
MS ..... *Multiple sclerosis*
NC1 ..... *Noncollagenous domain*
NK cell ..... *Natural killer cell*

NKT cell ..... *Natural killer T cell*
NTS ..... *Nephrotoxic serum nephritis*
OD ..... *Optical density*
PA ..... *Pennsylvania*
PAS ..... *Periodic acid–Schiff*
PBS ..... *Phosphate-buffered saline*
PE ..... *Phycoerythrin*
PR3 ..... *Proteinase 3*
RA ..... *Rheumatoid arthritis*
RLV ..... *Renal-limited vasculitis*
RNA ..... *Ribonucleic acid*
ROS ..... *Reactive oxygen species*
RPGN ..... *Rapidly progressive glomerulonephritis*
RRMS ..... *Relapse-remitting multiple sclerosis*
S1P ..... *Sphingosine 1-phosphate*
S1PR ..... *Sphingosine 1-phosphate receptor*
SEM ..... *Standard error of the mean*
SK ..... *Sphingosine kinase*
SLE ..... *Systemic lupus erythematodes*
SPMS ..... *Secondary progressive multiple sclerosis*
TCR ..... *T cell receptor*
TGF-β ..... *Transforming growth factor beta*
Th cell ..... *T helper cell*
TMB ..... *Tetramethylbenzene*
TNF-α ..... *Tumor necrosis factor* alpha
Treg ..... *Regulatory T cell*
TX ..... *Texas*
UK ..... *United Kingdom*
USA ..... *United States of America*
UTP ..... *Uridine triphosphate*

List of figures

List of tables

Zusammenfassung

Hintergrund: Derzeitige Therapiemöglichkeiten der rapid-progressiven Glomerulonephritis (RPGN) gehen häufig mit schweren Nebenwirkungen einher. Aus diesem Grund ist ein besseres Verständnis und Wissen über die Pathogenese dieser klinisch schwer verlaufenden Form der Glomerulonephritis (GN) unumgänglich um neue Ansätze für sicherere und effektivere Therapieformen in Zukunft gewährleisten zu können. Es konnte gezeigt werden, dass Sphingosin-1-phosphat und seine Rezeptoren (S1PR) einen Einfluss auf die Pathogenese mehrere Formen der GN haben. Daher wurde in dieser Arbeit die Wirkung eines selektiven S1P5 Rezeptor-Agonisten A-971432 im Rahmen des Mausmodells der nephrotoxischen Serumnephritis (NTS) genauer untersucht.

Methoden: Drei Tag nach der Immunisierung gegen Kaninchen-IgG, wurden acht bis zwölf Wochen alten, männlichen C57BL/6J Mäusen ein nephrotoxisches Kaninchen-anti Maus Serum injiziert. Ebenfalls am Tag der Immunisierung startete die tägliche intraperitoneale Behandlung mit dem selektiven S1PR-Agonisten A-971432, dem nicht-selektiven S1PR-Agonisten BAF-312 oder einer reinen Trägersubstanz, welche bis Tag 9 nach der NTS-Injektion fortgeführt wurde.

Resultate: Die Albuminurie in den mit A-971432 behandelten Mäusen zeigte vergleichbare Werte wie jene der mit BAF-312 oder mit der Trägersubstanz behandelten Mäuse. Außerdem konnten keine signifikanten Unterschiede bezüglich der humoralen Immunantwort festgestellt werden. Ebenfalls zeigten auch die PAS-Scores sowie tubuläre Zylinder in der Niere keine signifikanten Unterschiede zwischen den Gruppen, obwohl in den mit A-971432 behandelten Mäusen tendenziell weniger tubuläre Zylinder im Vergleich zu den beiden anderen Gruppen auffindbar waren. In die Niere infiltrierende $CD4^+$ T-Helfer Zellen zeigten sich in der BAF-312-Gruppe im Vergleich zur Trägersubstanzgruppe ($p = 0.014$) und der A-971432-Gruppe ($p = 0.014$) deutlich erniedrigt. Zusätzlich zeigten die mit BAF-312 therapierten Mäuse auch eine geringere Anzahl an $CD8^+$ T Helfer Zellen, welche sich allerdings nur im Vergleich zur A-971432-Gruppe ($p = 0.004$) als signifikant erwies. Infiltrierende $CD68^+$ und $Ly6G^+$ Zellen in der Niere waren in allen drei Gruppen in ähnlicher Anzahl vorhanden. Die CD1d-Tetramer Färbung in der Milz präsentierte eine erhöhte Anzahl an CD1d-positiven Natürlichen Killer T (NKT) Zellen in der BAF-312-Gruppe im Vergleich zur Trägersubstanzgruppe ($p = 0.017$) und der A-971432-Gruppe ($p = 0.014$).

Fazit: In unseren Versuchen zeigten die mit A-971432 behandelten Mäuse keine signifikanten Unterschiede in Bezug auf den Verlauf einer NTS im Vergleich zu der

Trägersubstanzgruppe. BAF-312 reduziert über den S1P1 Rezeptor die Infiltration von T Zellen in die Niere und erhöht die NKT Zell-Anzahl in der Milz.

Abstract

Background: Current treatment regimens of rapidly progressive glomerulonephritis (RPGN) are associated with severe adverse effects. Therefore, a greater understanding and knowledge of the pathogenesis in this aggressive clinical form of glomerulonephritis (GN) is important, ultimately aiming to achieve novel targets for further effective therapy options. Sphingosine 1-phosphate (S1P) and the receptors (S1PR) have been shown to be involved in multiple forms of GN. Thus, we evaluated the influence of a selective S1P5 receptor agonist, named A-971432, in a murine model of experimental nephrotoxic serum nephritis (NTS).

Methods: Three days after immunization against rabbit IgG, NTS was induced in eight to twelve weeks old male C57BL/6J mice. Starting on the same day as immunization, a daily intraperitoneal treatment with selective S1P5 receptor agonist A-971432, the nonselective S1P1 and S1P5 receptor agonist BAF-312 or vehicle was performed until day 9 after NTS induction.

Results: Albuminuria in mice treated with A-971432 was comparable to mice which received BAF-312 or vehicle. Furthermore, no significant differences in humoral immune response were found. The three groups did not differ significantly in terms of their evaluated PAS-score or tubular cast formation in the kidney, although a tendency of decreased numbers of tubular casts in mice treated with A-971432 was observed. Infiltrating $CD4^+$ cells into the kidney were increased in the BAF-312-treated mice compared to vehicle-treated ($p = 0.014$) as well as to the A-971432-treated mice ($p = 0.014$). Additionally, mice receiving BAF-312 therapy also showed a decreased number of $CD8^+$ cells in contrast to mice with A-971432 therapy ($p = 0.004$). Differences of infiltrating innate immune cells into the kidney expressing CD68 and Ly6G were not detected. The CD1d-tetramer staining in spleen presented an increased number of natural killer T (NKT) cells in the BAF-312-treated mice compared to vehicle-treated ($p = 0.017$) and A-971432-treated mice ($p = 0.014$).

Conclusion: Treatment of A-971432 did not improve the course of NTS compared to the vehicle group after short time treatment. BAF-312 decreases T cell infiltration into the kidney probably by S1P1 receptor, whereas NKT cells increase in the spleen.

1 Introduction

1.1 Kidney and glomerular filtration

1.1.1 Anatomy

The kidney, an organ arranged as a pair, is situated in the retroperitoneal space directly beneath the diaphragm (1). Characterized by a bean-shaped form, the kidney is approximately 12 cm long, 6 cm wide, 2,5 cm thick and weighs between 250 and 300g in human adults. The parenchyma is divided into an outer renal cortex covered by a thin fibrous capsule and an inner renal medulla, which is composed by a dozen of renal pyramids. These cone-shaped structures together with cortical tissue at its base and at the sites form a renal lobe. The tips of each renal pyramids are called renal papilla. They collect the urine from the renal lobes and transmit into a minor calyx. Several minor calyces combine to one major calyx, which in turn build the renal pelvis with other major calyces and subsequently the ureter (2).

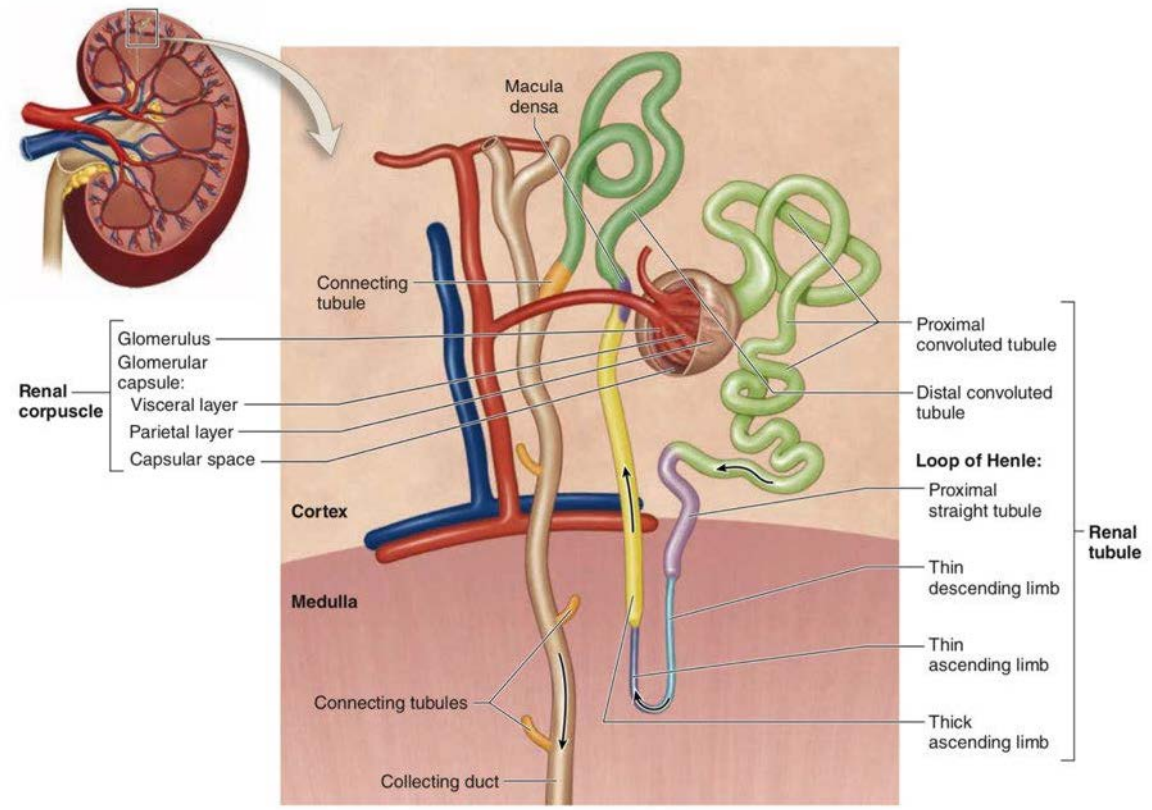

Figure 1: Structure of nephron

From: Mescher AL. Junqueira's Basic Histology: Text and Atlas, Fourteenth Edition. McGraw-Hill Education; 2015 (2).

The functional unit of the kidney is called nephron and is found approximately one to four million times in each organ (Figure 1) (2). A nephron is composed by a corpuscle and a long renal tubule system consisting of a proximal tubule, loop of Henle or nephron loop, a distal tubule and a connecting tubule joining the nephron with the collecting duct, which in turn merges into the renal papilla (3).

1.1.2 Functions

The kidney has several important functions. Besides the secretion of renin and erythropoietin, as well as the conversion of the prohormone vitamin D to its active form, specialized epithelial cells of the nephron and the collecting duct are crucial for the adequate excretion of metabolites, surplus water and electrolytes in urine (4). This process begins in the renal corpuscle consisting of a bundle of glomerular capillaries and enveloped by the glomerular (Bowman) capsule, which is structurally divided into an outer or parietal layer and an inner or visceral layer. The last mentioned is constructed by complex epithelial cells, called podocytes, covering the capillaries. Between the fenestrated endothelial cells of the capillaries and the podocytes, the glomerular basement membrane (GBM) is found. The basic structure of this thick layer, formed by a network of mainly collagen-IV, laminin, fibronectin and integrin molecules, is the essential component of the blood-urine barrier. The space receiving this so-called primary urine, filtered by the capillaries and the visceral layer, is called capsular (Bowman) space. In addition to the endothelial cells and podocytes, another type of cells, called mesangial cells (MCs), is found in the renal corpuscles. The physiological functions of MCs are the structural maintenance of the glomeruli as well as the participation in regulating glomerular filtration. Furthermore, they are able to secrete a broad range of cytokines as part of local immune response mechanisms (2,5).

The normal range of this glomerular filtration rate (GFR) is 180 L per day or, adjusted for body surface area, 120 mL/min/1,73m^2. After passing the glomerulus, the filtrate moves to the tubules where tubular reabsorption and secretion takes place building secondary or end urine, which amounts approximately 1,5 L per day (6).

Due to the physiological decrease of GFR in older age or pathologically in case of various renal diseases, the Kidney Disease: Improving Global Outcomes (KDIGO) clinical practice guidelines strongly recommend the determination of GFR to evaluate kidney function (7). The basic principle of this assessment is to measure the quantitative balance of in- and output concentration of an indicator substance in order to establish the flow rate in the kidney. For example, inulin can be used as such a marker. This freely filtered polysaccharide is neither

reabsorbed, secreted nor newly synthesized by the renal tubules, subsequently it can be concluded that glomerular filtration (input) is directly proportional to the excretion (output) in urine of this substance (Equation 1) (4,8).

$$filtrated\ inulin/time\ =\ excreted\ inulin/time$$

Equation 1: Measurement of inulin clearance for assessing GFR (I)

Assuming that the quantity per time is equal to (volume per time) times concentration and furthermore the concentration of a freely filtered substance is practically equal in plasma as well as in the filtrate, equation 2 can be used.

$$GFR \cdot P = \dot{V}\ \cdot U$$

Equation 2: Measurement of inulin clearance for assessing GFR (II) GFR = glomerular filtration rate; P = filtrated inulin in plasma [g/L]; V = urine time volume [mL/min]; U = concentration of inulin in the urine [g/L]

After transforming equation 2, the formula for the direct calculation of the inulin clearance or rather GFR results (Equation 3).

$$GFR = \dot{V} \cdot U \div P$$

Equation 3: Measurement of inulin clearance for assessing GFR (III) GFR = glomerular filtration rate [mL/min]; P = filtrated inulin in plasma [g/L]; V = urine time volume [mL/min]; U = concentration of inulin in the urine [g/L]

The inulin is normally applied intravenously and its concentration in plasma and urine is measured photometrically. For the determination of urine volume per minute, the urinary bladder is initially emptied and a 24-hours urine collection is executed. The urine volume per minute results from the division of the collected urine volume divided by the time interval of urine collection (usually 24 hours) (4).

The external infusion of inulin is a time-consuming procedure and therefore another indicator such as creatinine, a product from muscle and protein metabolism excreted constantly in urine, is rather used to measure GFR. Although endogenous creatinine is partly secreted in renal tubules, endogenous creatinine has been approved as a significant marker for the renal filtration capacity (9).

As the urine sampling in clinical practice is associated with considerable time and effort, empiric formula requiring serum creatinine value, age and sex have been developed for the estimation of GFR. In current clinical practice, KDIGO clinical practice guidelines recommend the use of the Chronic Kidney Disease Epidemiology Collaboration (CKD-EPI)

Creatinine equation for the calculation of this so-called estimated GFR (eGFR) (Equation 4) (7).

$$eGFR = 142 \cdot \min\left(\frac{S_{cr}}{\mathrm{k}}, 1\right)^{\alpha} \cdot \max\left(\frac{S_{cr}}{k}, 1\right)^{-1.200} \cdot 0{,}9930^{age}$$

Equation 4: CKD-EPI creatinine equation: eGFR = estimated glomerular filtration rate [mL/min/1,73^2]; S_{cr} = standardized serum creatinine [mg/dL]; k = 0,7 (females) or 0,9 (males); α = -0.24l (females) or -0,302 (males); min = indicates the minimum of S_{cr}/k or 1; max = indicates the maximum of S_{cr}/k or 1; age = years

1.2 Glomerulonephritis

1.2.1 Definition, epidemiology and systematic classification

Glomerulonephritis (GN) is a term used to summarize various immune-mediated diseases in the kidney which cause inflammatory changes within the glomerulus (10,11). Most patients with GN develop chronic kidney disease (CKD) and are consequently at increased risk of premature cardiovascular disease and progressive kidney failure (12).

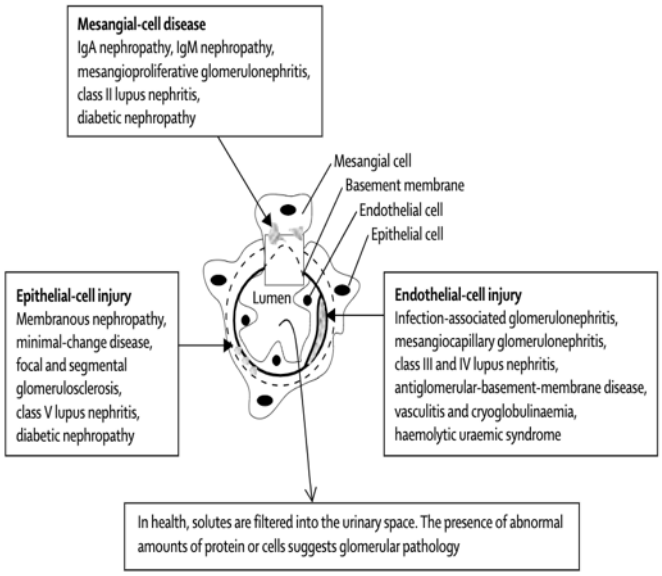

Figure 2: Cellular location of glomerular injury during glomerulonephritis

From: Chadban S, Atkins R. Glomerulonephritis. Lancet. 2005;365(9473):1797–806 (11).

Due to the variety of these diseases, GN can be classified by its aetiology, pathology or clinical symptoms.

According to the aetiology, GN may occur as a primary kidney disease (aetiology unknown, generally assumed to be an autoimmune manifestation) or be a component of a systemic disorder such as severe autoimmune (e.g. systemic lupus erythematosus), infectious, malignant or metabolic diseases (secondary GN) (11,13).

The histopathologic forms of GN can be divided by their location of the glomerular damage (Figure 2). The pathologic description also considers glomerular involvement. It can be distinguished between a diffuse (all glomeruli are affected by the inflammation) or focal (only some glomeruli are affected) distribution pattern. Within an injured glomerulus the capillaries can be involved segmentally or globally. Furthermore, cellular proliferation can be found in some forms of GN.

However, the most effective tool for the clinicians remains the classification according to the clinical presentation (Table 1) (11,14). Besides asymptomatic urinary abnormalities defined as a microscopic haematuria and less than 150 mg protein per day in the urine, a further distinction can be drawn between nephrotic and nephritic syndrome (13). The presentation of nephrotic syndrome is usually characterized by hypalbuminaemia, oedema and dyslipidaemia. Common causes in adults are diabetic nephropathy, focal segmental glomerulosclerosis, membranous GN and membranoproliferative GN (15).

Nephritic syndrome in turn is a clinical syndrome characterized by haematuria, proteinuria, water and salt retention as well as hypertension. IgA nephropathy, lupus nephritis, acute proliferative GN due to a post-streptococcal GN, or a crescentic GN (CGN) in the context of a rapidly progressive glomerulonephritis (RPGN) (Chapter 1.2.2) are the most frequent diseases resulting in nephritic syndrome (16).

Table 1: Classification according to clinical presentation (adapted from (11–14))

Asymptomatic urinary abnormalities	Microscopic haematuria > 2-3 red blood cells/HPF Proteinuria < 150mg/d Not accompanied by hypertension
Nephrotic syndrome	Proteinuria > 3,5g/d Hypalbuminaemia, hyperlipidaemia Oedema
Nephritic syndrome	Recent onset of haematuria and proteinuria < 3g/d Renal impairment and salt and water retention which can be accompanied by hypertension
Rapidly progressive glomerulonephritis	Progression to renal failure over days to weeks, in most cases in the context of a nephritic presentation, typically associated with the pathological finding of extensive glomerular crescent formation on renal biopsy
Chronic glomerulonephritis	Persistent proteinuria with or without haematuria and slowly progressive impairment of renal function

1.2.2 Rapidly progressive glomerulonephritis (RPGN)

1.2.2.1 Definition and epidemiology

RPGN cannot be classified as a specific renal disease but rather is an aggressive clinical form of GN that can have many different aetiologies and pathogenic mechanism (Table 1). RPGN is characterized by an extensive loss of excretory renal function over weeks to month with a rapid reduction in GFR and CGN as the principal histological finding. This description refers to the crescentic extracapillary proliferation within the Bowman's space that is due to

the rupture of glomerular capillaries that in turn allows cellular and humoral inflammatory mediators to migrate into this filtration space (17,18).

With an incidence of less than 1/100000/year, RPGN is relatively rare (19). Nevertheless, a rapid diagnosis, which must include accurate subclassification, is crucial to start adequate therapy and consequently to improve renal survival as well as the optimum patient outcome (17,18).

1.2.2.2 Classification, aetiology and pathogenesis

According to Couser, RPGN can be divided into three major groups on the basis of immunopathologic studies. These include anti-glomerular basement membrane antibody (anti-GBM), immune complex-induced and pauci-immune GN, which is often associated with antineutrophil cytoplasmic autoantibodies (ANCA) (18). The essential criteria for this classification are the incidence of immunoglobulins (Ig) as well as their distribution (capillary, mesangial), pattern (linear, granular) and composition (IgA-, IgG- or IgM-dominated). Furthermore, these three categories can be subclassified based on clinical, pathologic and serologic findings (17).

1.2.2.3 Type 1 (Anti-GBM glomerulonephritis)

Approximately 20% of the patients diagnosed with RPGN suffer from type 1 (18), also called anti-GBM GN, which is classified as an immune-complex small vessel vasculitis in the Revised International Chapel Hill Consensus Conference Nomenclature of Vasculitides (Figure 3 and Table 2) (20). Histologically this form of RPGN is characterized by linear depositions of IgG along the GBM (21,22).

In some patients autoantibodies are also deposited on the alveolar basement membrane causing pulmonary haemorrhage. In case of involvement of the GBM as well as the alveolar basement membrane, the term “Goodpasture’s disease” can be used to describe this type of RPGN referring to Ernest Goodpasture. The last mentioned American pathologist described for the first time a fatal case of GN and lung haemorrhage (23). Although his description probably resembled more an ANCA-associated vasculitis than anti-GBM disease due to the additional intestinal and splenic inflammation, the term “Goodpasture’s disease” has been maintained (24,25). The term “anti-GBM GN” will be used in the following chapters when referring especially to kidney involvement and “anti-GBM disease” when the kidney and the lungs are affected.

A bimodal age distribution of anti-GBM patients has been observed. While men in their thirties were more likely to develop kidney and lung disease, women tended to have an increased risk of isolated anti-GB GN during the sixth or seventh decades (25,26).

The causes for the autoantibody synthesis remain to be further investigated, nevertheless a possible infectious association with influenza A responsible for seasonal or geographical onsets of anti-GBM disease has been reported (27). Cigarette smoking and inhalation of hydrocarbons has also been shown to trigger this disease (28,29).

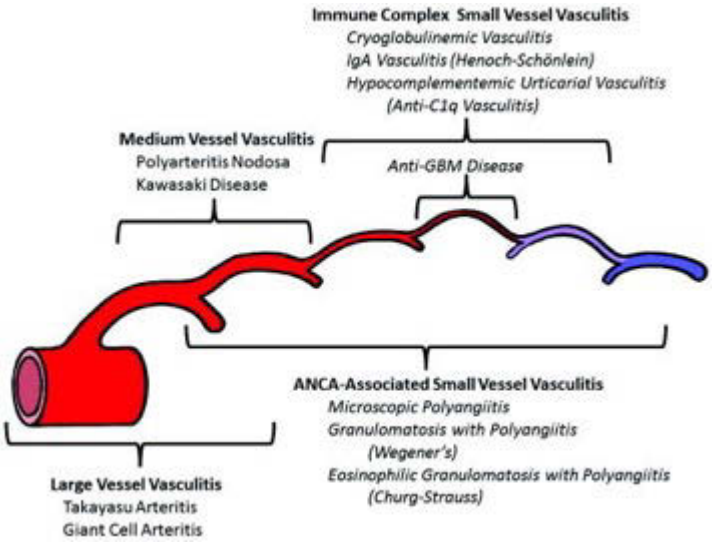

Figure 3: Classification of large vessel vasculitis, medium vessel vasculitis and small vessel vasculitis

From: . Jennette JC, Falk RJ, Bacon PA, Basu N, Cid MC, Ferrario F, et al. 2012 Revised International Chapel Hill Consensus Conference Nomenclature of Vasculitides. Arthritis Rheumatism. 2013;65(1):1–11 (20).

Next to the environmental aspects, anti-GBM disease is strongly associated with certain human leukocyte antigen (HLA) genes. Up to 80% of patients with anti-GBM disease are carriers of the HLA-DR2 haplotype gene. A susceptible association with DRB1*1501 and DRB1*0401 alleles has been detected as well as a protective association with DRB1*07 alleles (30). However, these identified susceptibilities are common in most populations and associated with other autoimmune diseases such as multiple sclerosis (MS) (25).

Lerner et al. already in 1967 clearly demonstrated the development of CGN in nonhuman primates by injecting them with antibodies gained from the kidneys of patients with anti-GBM antibodies (31). Human anti-GBM antibodies are usually of the IgG (rarely IgM or IgA) class and characterized by high affinity (26,32). The principle target of the autoimmune response was detected to be the noncollagenous (NC1) domain of the $\alpha 3$ chain of type IV collagen ($\alpha 3$[IV]NC1). This autoantigen is found in the basement membrane of the kidney and lung, as well as, to a lesser extent, of the cochlea and the eye explaining the clinical presentation of the disease (33,34). In this selected basement membranes, $\alpha 3$, $\alpha 4$ and $\alpha 5$ monomer chains fuse together into a triple helical protomer (Figure 4). The collagen network

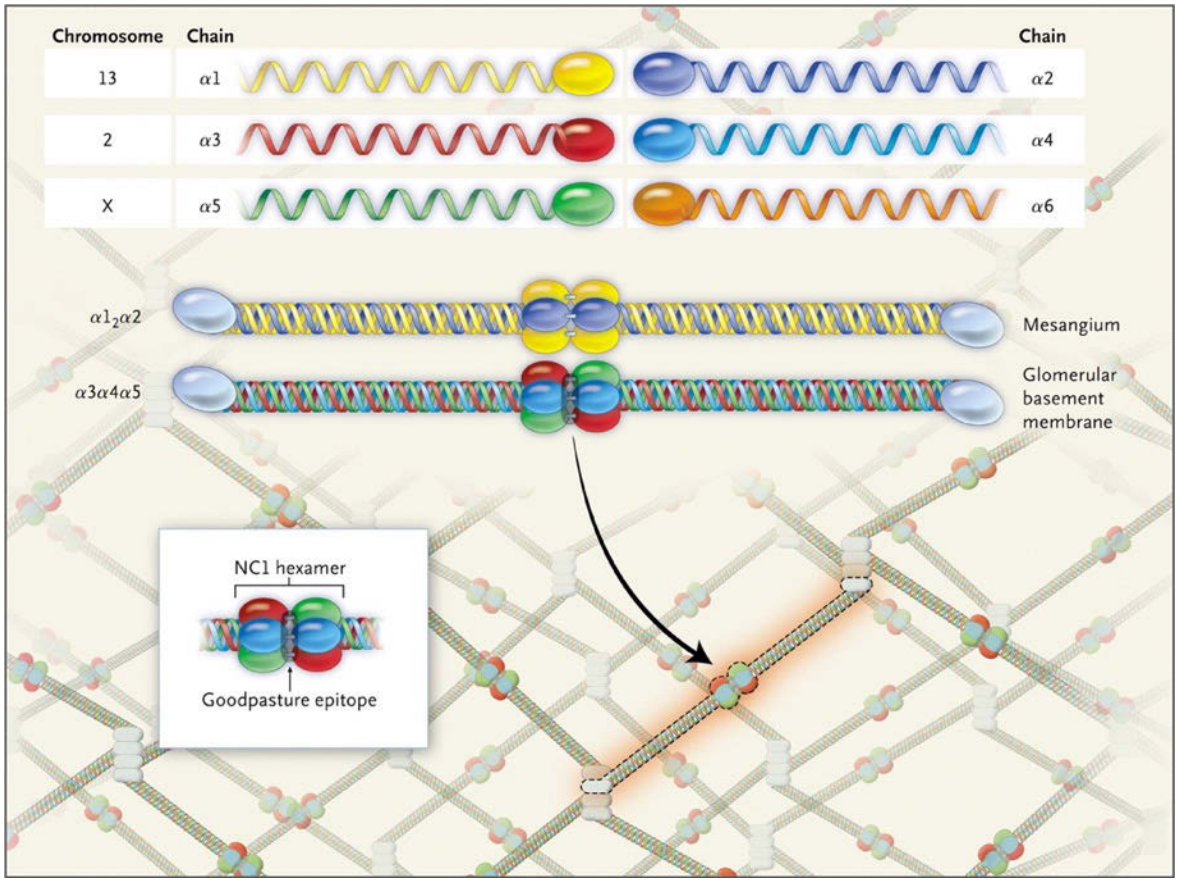

Figure 4: Structure and composition of type IV collagen

From: Salant DJ. Goodpasture's Disease — New Secrets Revealed. New Engl J Medicine. 2010;363(4):388–91 (39).

is then created by connecting these triple helices to one another at their ends. In this process, two protomers are linked together through C-terminal NC1 domains, forming an NC1 hexamer (35). The detection of two principle autoantibody epitopes within the α3[IV]NC1domain by Netzer et al., have been termed E_A and E_B (36). In the naïve GMB, they are usually unreachable for the antibodies to bind unless a disjunction of the NC1 hexamer occurs (21).

According to Pedchenko et al., all patients with anti-GBM disease seem to have autoantibodies directed against α3NC1, nevertheless a part of them shows to build autoantibodies reacting to α4 and α5 chains as well. The authors used the term "conformeropathy" to describe the autoimmune-induced Goodpasture's disease considering that an impaired quaternary structure of the α345NC1 hexamer induces a pathogenic conformational change that in turn triggers an autoimmune response. Furthermore, he demonstrated that anti-GBM antibodies bound to specific epitopes in the region E_A in the α5NC1 and in regions E_A and E_B in the α3NC1 monomer, but there was no binding to the native crosslinked α345NC1 hexamer (37). These results would reinforce the finding of several associated environmental factors, including viruses, smoking and hydrocarbons, that

expose the pathogenic epitopes by changing the collagen structure (35,37,38). However, it remains unknown whether the conformational change in the NC1 hexamer is due to environmental events or to the autoantibody itself that may cause structural disturbance and subsequently initiate the autoimmune response (38,39).

In addition to the humoral responses, T cells seems also to play a role in the pathogenesis of anti-GBM disease. Animal studies, conducted by Wu et al., demonstrated that the induction of α3(IV)NC1-specific $CD4^+$ T cells into pertussis-toxin primed naïve syngeneic rats was sufficient to induce GN in the recipients. Animals developed sever proteinuria/albuminuria and histopathology revealed a CGN (40). Also, in case of transferring Goodpasture's disease by the injection of α3(IV)NC1 heterodimers in B-cell-deficient mice, renal injury was detected (41). The involvement of cell mediated immunity in the pathomechanism of anti-GBM GN is supported by histological evaluation in RPGN patients observing T lymphocytes in the kidneys (42). The HLA association described above also suggest a need for T cells to contribute to the autoimmune response (25). Because of findings of these autoreactive T cells in healthy individuals along with low-level natural autoantibodies, a suggestion has been made that in anti-GBM patients, tolerance to the α3[IV]NC1 domain hasn't been completely reached during immunological development in the thymus (43).

Complement activation as well as interleukin-12 (IL-12) and interferon-γ (INF-γ) secretion also play a role in the pathomechanism of anti-GBM disease together with the function of macrophages and neutrophils leading to disruption of the filtration barrier and Bownman's capsule with resultant proteinuria, intestinal nephritis and fibrosis (35,44–46).

1.2.2.4 Type 2 (Immune complex-induced glomerulonephritis)

Immune complex-induced GN includes approximately 40% of all patients with RPGN (18). This type 2 of GN is histologically characterized by granular deposits of immunoglobulins in the glomerular mesangium and capillaries. It less frequently shows crescent formation within the Bowman's space as compared to anti-GBM GN or ANCA-associated GN. The extent of crescents correlates directly with the severity of the disease. Furthermore, the prognosis strongly depends on the underlying cause (17).

Immune complexes are produced when an antibody binds to a soluble antigen. Normally, such complexes are removed very quickly by red blood cells expressing complement receptors and by phagocytosis. Nevertheless, this clearance mechanism can fail when the production of immune complexes exceeds its capacity or when there are deficiencies in the

clearance system leading to injury in small blood vessels in organs such as the kidney and the skin (Table 2).

One cause resulting in immune complexes in the kidney as well as in other tissues, is systemic lupus erythematosus (SLE). This chronic autoimmune disease, characterized by the autoantibody production against nuclear antigens (anti-nuclear antibodies = ANAs) produces a large amount of small immune complexes that are subsequently deposited in the walls of small blood vessels in the renal GBM leading to lupus nephritis. Other small vessels in joints and other organs can also be affected. This leads to the activation of phagocytosis as well as the complement pathway. Some hereditary deficiencies in complement proteins, e.g. C1q or C4, are strongly associated with development of SLE in humans. In consequence, immune complexes cannot be cleared sufficiently conducting to tissue damage (47).

Among other causes resulting in immune complex-induced GN, postinfectious GN must be mentioned, which manifests after an extrarenal infection. Especially streptococci can induce glomerular injury after a few days or a couple of weeks and approximately 15% of infected patients, especially children, develop GN (48,49).

Further causes are primary renal lesions such as IgA nephropathy or membranoproliferative GN (18). IgA nephropathy is the most common form of primary GN, typically concerning young adults but also children and older people can be affected. The prevalence of IgA nephropathy varies geographically. Whereas in East Asia 32 to 54% of all primary GN account for IgA nephropathy, European countries show a prevalence rate of 10 to 35%. IgA nephropathy is characterized by the production of circulating galactose-deficient IgA1, probably induced by genetic and environmental factors. Th galactose-deficient region of IgA1 is then recognized by specific anti-glycan antibodies forming immune complexes. The deposition of these last-mentioned in the kidney results in a mesangial cell proliferation as well as in a local production of proinflammatory cytokines leading to

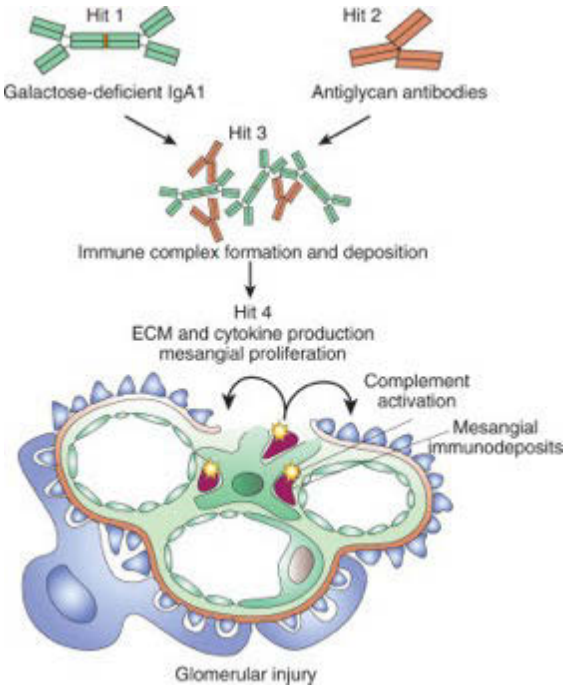

Figure 5: The multihit pathogenesis model of IgA nephropathy

From: Magistroni R, D'Agati VD, Appel GB, Kiryluk K. New developments in the genetics, pathogenesis, and therapy of IgA nephropathy. Kidney Int. 2015;88(5):974–89.

glomerular injury (50,51). Various studies have shown that not all patients with increased galactose-deficient IgA1 levels develop IgA nephropathy, but further triggers are needed for the production of anti-glycan antibodies and consequently the formation of immune complexes and glomerular injury (52,53). This “multihit” pathogenesis model has been illustrated by Magistroni et al. in figure 5 (50).

Membranoproliferative GN (MPGN), also called mesangiocapillary GN, has an incidence of 0.2/100’000/year and especially affects children and young adults (54,55). Primary or idiopathic MPGN is classified into three types, whereas type 1 accounts for the most common form. MPGN type 1 is characterized by immune-complex-mediated and complement-mediated subendothelial deposits in the glomeruli (56). The formation of immune complexes results due to autoimmune diseases, including among others systemic lupus nephritis and Sjögren’s syndrome, or monoclonal gammopathies (57–59). These immune complexes in turn provoke the activation and deposition of complement factors along the capillaries leading to acute glomerular injury. Furthermore, the influx of inflammatory cells and the production of proinflammatory cytokines results in a disruption of the glomerular endothelial cells as well as of the GBM. The following reparative phase is characterized by the building of a new GBM, entrapping the immune complexes and complement proteins in the subendothelial space. Under electron microscopy, this duplicated GBM appears like so-called tram tracks, which is a typical feature or MPGN type 1. Additionally to type 1, type 3 shows subepithelial deposits and type 2 is characterized by complement deposits, also termed dense deposits, in the GBM. Secondary forms of MPGN are usually due to a chronic infections such as hepatitis C leading to an immune-mediated MPGN (56).

1.2.2.5 Type 3 (Pauci-immune glomerulonephritis)

Observations of patients with the histological finding of CGN, in the absence of immunoglobulins in the glomeruli, neither in form of anti-GBM nor as immune complexes, have been made (60). Approximately 80-90% of these patients with this so-called pauci-immune GN (lat.: pauci = few, little) have circulating ANCAs, which are directed against the granules of neutrophils. These antibodies show an antigen specificity for myeloperoxidase (MPO-ANCA) or proteinase 3 (PR3-ANCA). ANCA-associated GN can be limited to the kidneys, but over 75% of all cases goes together with systemic vasculitis (61,62). According to 2012 Revised International Chapel Hill Consensus Conference Nomenclature of Vasculitides, ANCA-associated vasculitis are necrotizing vasculitides with

few or no immune deposits, predominantly affecting small vessels (i.e., capillaries, venules, arterioles, and small arteries). Referring to pathological and clinical aspects, ANCA-associated vasculitis can be classified into microscopic polyangiitis (MPA), granulomatosis with polyangiitis (GPA), eosinophilic granulomatosis with polyangiitis (Churg-Strauss) (EGPA) and single-organ ANCA-associated vasculitis such as renal-limited vasculitis (RLV) with pauci-immune GN (Figure 3). In contrast to MPA, GPA usually shows granulomatous inflammation involving the upper and lower respiratory tract. In addition to the eosinophil-rich and necrotizing granulomatous inflammation in the respiratory tract, EGPA is often associated with asthma and eosinophilia (Table 2) (20).

Table 2: Definitions for vasculitides adopted by the 2012 International Chapel Hill Consensus Conference on the Nomenclature of Vasculitides (CHCC2012) (adapted from (20))

CHCC2012 name	CHCC2012 definition
ANCA-associated vasculitis (AAV)	Necrotizing vasculitis, with few or no immune deposits, predominantly affecting small vessels (i.e., capillaries, venules, arterioles, and small arteries), associated with myeloperoxidase (MPO) ANCA or proteinase 3 (PR3) ANCA. Not all patients have ANCA. Add a prefix indicating ANCA reactivity, e.g., MPO-ANCA, PR3-ANCA, ANCA-negative.
Microscopic polyangiitis (MPA)	Necrotizing vasculitis, with few or no immune deposits, predominantly affecting small vessels (i.e., capillaries, venules, or arterioles). Necrotizing arteritis involving small and medium arteries may be present. Necrotizing glomerulonephritis is very common. Pulmonary capillaritis often occurs. Granulomatous inflammation is absent.
Granulomatosis with polyangiitis (GPA)	Necrotizing granulomatous inflammation usually involving the upper and lower respiratory tract, and necrotizing vasculitis affecting predominantly small to medium vessels (e.g., capillaries, venules, arterioles, arteries and veins). Necrotizing glomerulonephritis is common.
Eosinophilic granulomatosis with poly angiitis (Churg-Strauss) (EGPA)	Eosinophil-rich and necrotizing granulomatous inflammation often involving the respiratory tract, and necrotizing vasculitis predominantly affecting small to medium vessels, and associated with asthma and eosinophilia. ANCA is more frequent when glomerulonephritis is present.
Immune complex vasculitis	Vasculitis with moderate to marked vessel wall deposits of immunoglobulin and/or complement components predominantly affecting small vessels (i.e., capillaries,

	venules, arterioles, and small arteries). Glomerulonephritis is frequent.
Anti–glomerular basement membrane (anti-GBM) disease	Vasculitis affecting glomerular capillaries, pulmonary capillaries, or both, with GBM deposition of anti-GBM autoantibodies. Lung involvement causes pulmonary hemorrhage, and renal involvement causes glomerulonephritis with necrosis and crescents.

As mentioned above, glomerular injury in all forms of systemic ANCA-associated vasculitis as well as in RLV is characterized by pauci-immune necrotizing and crescentic GN. The acute lesion in glomeruli and other vessels in the body is a vessel wall necrosis which liberates components of the plasma such as coagulation factors into the necrotic zone and activates the coagulation cascade to produce fibrin creating a fibrinoid necrosis (63).

Besides the clinicopathological classification, the serological results (e.g. PR3-ANCA, MPO-ANCA, ANGA-negative) can be useful to determine genetic associations, typical disease characteristics as well as the prognosis and the response to therapy (64). PR3, a small neutrophil serine protease, is stored in primary granules, secretory vesicles and specific granules of neutrophils. Especially during neutrophil activation and apoptosis, PR3 is expressed on the cell surface (64,65). The function of MPO, a member of the superfamily of mammalian haem peroxidase, is the production of reactive oxygen species (ROS) from the substrate H_2O_2 contributing to the degradation of the phagocytized pathogens. Additionally, MPO-derived oxidants have been detected to be involved in tissue damage in many acute and chronic inflammatory diseases.

According to the epidemiology, PR3-ANCA vasculitis is more widespread in Northern European and American countries and Australia whereas MPO-ANCA is more frequently found in Southern Europe and Asia (Table 3). The age at diagnosis for PR3-ANCA vasculitis is usually earlier (45-55 years) than for MPO-ANCA vasculitis (60-65 years). Various genetic polymorphism have been reported to be associated with ANCA vasculitis such as for example HLA-DP for PR3-ANCA vasculitis and HLA-DQ for MPO-ANCA vasculitis. Upper airway involvement in PR3-ANCA vasculitis is more frequent than in MPO-ANCA whereas renal injury is more common in the last-mentioned type of vasculitis (64). Furthermore, PR3-ANCA is associated with GPA and MPO-ANCA with MPA, even though MPO-ANCA can occur in GPA and PR3-ANCA in MPA as shown in table 4 (66).

Table 3: Differences between PR3-ANCA vasculitis and MPO-ANCA vasculitis (adapted from (64,67))

Feature	PR3-ANCA vasculitis	MPO-ANCA vasculitis
Epidemiology	Frequent in Northern European and American countries and Australia	Frequent in Southern Europe and Asia
Usual age at diagnosis	45-55 years	60-65 years
Genetic associations	HLA-DP SERPINA1 (encoding a1-antitrypsin) PRTN3 (encoding PR3)	HLA-DQ
Pathology	Granuloma and vasculitis	Vasculitis and fibrosis
Organ involvement	Frequent upper airway involvement and lung nodules High number of organs involved	Frequent renal involvement and pulmonary fibrosis
Prognosis	Increased risk of relapse	Increased rate of initial treatment failure Increased long-term risk of end-stage renal disease
Response to therapy	Rituximab superior to cyclophosphamide for remission induction PR3-ANCA titre might guide therapy after rituximab	Similar response to rituximab and cyclophosphamide

Table 4: Disease associations of PR3-ANCA and MPO-ANCA (adapted from (66))

Disease entity	Sensitivity of PR3-ANCA (%)	MPO-ANCA (%)
Granulomatosis with polyangiitis (GPA)	66	24
Microscopic polyangiitis (MPA)	26	58
Idiopathic crescentic GN	30	64
Eosinophilic granulomatosis with poly angiitis (Churg-Strauss) (EGPA)	<5	40

Data have indicated that ANCA specificity can predict prognosis as well as the response to therapy among patients with ANCA vasculitis more effectively than clinicopathological classifications systems such as the CHCC 2012 definitions. The risk to relapse in PR3-ANCA-positive patients is twofold higher compared with MPO-ANCA-patients and respond more likely to rituximab than to cyclophosphamide (Table 3). ANCA specificity seems to be the best predictive model to classify ANCA-vasculitis in clearly defined groups (63,64,67,68).

In vitro models, animal models and clinical studies have demonstrated the pathogenic potential of ANCAs. The presence of ANCAs in 80-90% of patients with pauci-immune GN support this thesis that ANCAs are causing the disease. However, there are still doubts about

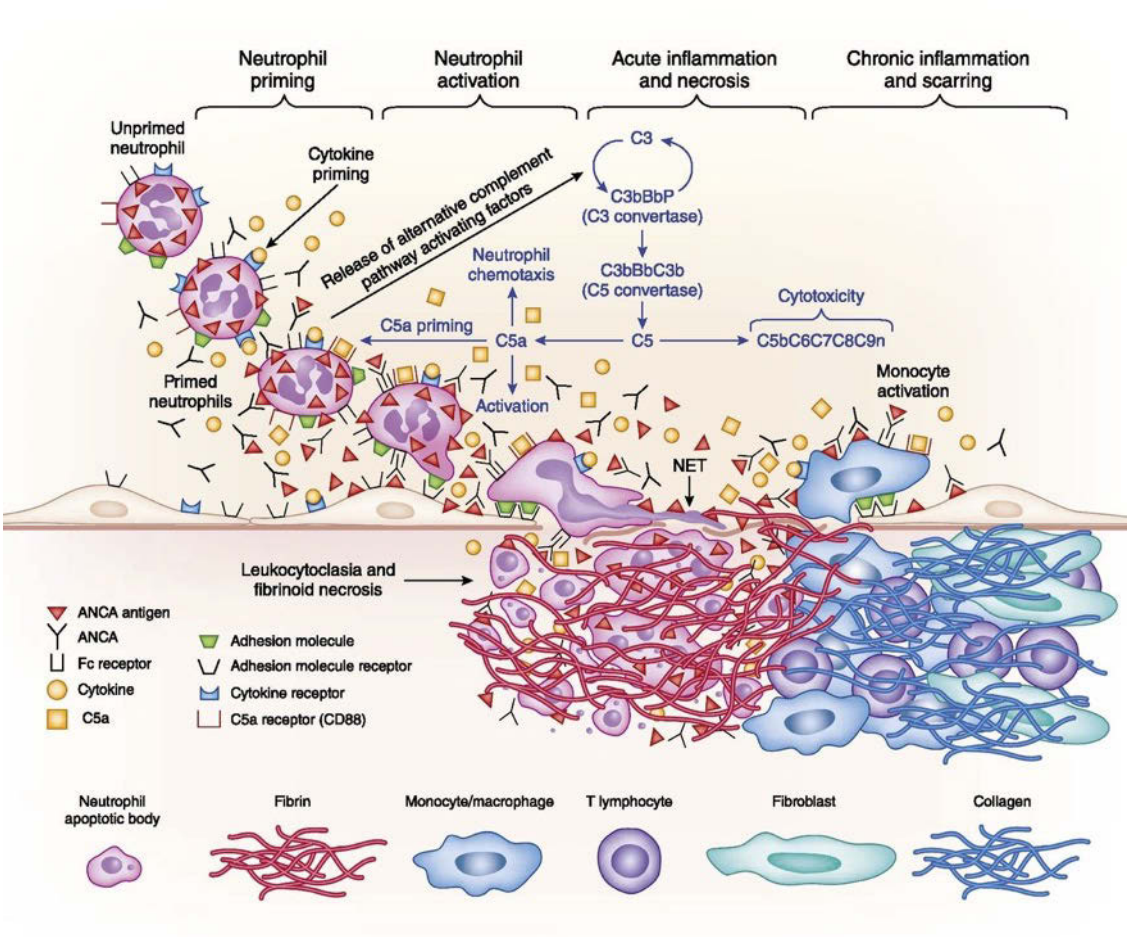

Figure 6: Pathogenesis of vascular lesions in ANCA vasculitis and GN

From: Jennette JC, Nachman PH. ANCA Glomerulonephritis and Vasculitis. Clin J Am Soc Nephro. 2017;12(10):1680–91(63).

the causality because of the ANCA-negative patients presenting an ANCA vasculitis disease phenotype. This could be explained by the fact that there may be further autoantigen epitopes that are not yet detected in current serological assays for ANCA (63,69,70).

Jennette et al. demonstrated, based on *in vitro* experiments, *in vivo* animal model experiments and clinical observation, a possible pathogenic mechanism induced by ANCAs (Figure 5). At the beginning, primed human neutrophils express ANCA antigens on their surfaces and inside the cell. ANCA-activated neutrophils penetrate subsequently the vessel walls by releasing inflammatory mediators and undergoing NETosis (63). NETosis is a strategy of neutrophils, found out by Brinkman et al., which release granule proteins and chromatin creating these so-called neutrophil extracellular traps (NETs) that are then able to bind and kill bacteria (71). At the damaged site of the vessel walls, coagulations factors of the plasma enter the necrotic zone and, in an activated state, produce fibrin leading to fibrinoid necrosis in vessels in tissue and crescents in glomeruli. A few days later,

macrophages and lymphocytes infiltrate the acute inflammation and start the scarring process.

Neutrophil priming in patients can occur during a simultaneous synergistic infection, for example a viral respiratory infection. Within one to two weeks, each localized vascular lesion caused by this described process transforms from an acute into a chronic phase. Nevertheless, numerous new acute lesions in many different vessels make progression until patients reach remission (63).

In summary, the initial cause for the production of ANCA remains still unclear. Different HLA molecules could be involved in the autoimmune response as well as overexpression of the MPO and PRTN3 genes in patients with active ANCA vasculitis compared with patients in remission or healthy controls (72).

NETosis could also play an important role in the pathogenesis of ANCAs. By releasing granule proteins and chromatin, including PR3 and MPO, the resulting extracellular network is subsequently more reachable for the immune system allowing them to induce an autoimmune ANCA response (73).

1.2.2.6 Treatment

This part will describe the general principles of the therapy of RPGN. Crucial for the treatment are the immunosuppressive substances with the aim of counteracting the pathological inflammatory processes in the kidneys and other organs (74).

In the year 1976, Lockwood et al. were the first who described a combination of intensive plasma-exchange, cytotoxic drugs and steroids as therapy regimen of anti-GBM GN (75). This treatment remains the standard recommendation for type 1 RPGN according to the latest KDIGO clinical practice guidelines (7). A daily plasmapheresis aiming to achieve a rapid reduction of antibody levels in the blood should be continued for 14 days or until the anti-GBM antibodies are completely filtered from the blood. Cyclophosphamide, an immunosuppressive drug acting as an inhibitor of proliferation of lymphocytes by impairing DNA synthesis (47), is given orally at a daily dose of 2-3 mg/kg for two to three months. Nevertheless, cyclophosphamide has a high risk of toxic effects, including leukopenia, severe infections, cancer and infertility (76–79). A small study showed that rituximab may be used as an additional or alternative therapy to cyclophosphamide. It is applied at a dose of 375 mg/m^2 of body-surface area per week for four weeks (80). Rituximab is an anti-CD20 monoclonal antibody, initially developed for the treatment of B-cell lymphomas. By binding to CD20 on the surface of B-cells, rituximab induces apoptosis and depletion of the

lymphocytes for several months (47). Regarding corticosteroids, 1 mg/kg oral prednisolone per day is used and a reduction of the dose to 20 mg within six weeks should be executed followed by a constant tapering until complete cessation at six to nine months (25).

The Euro-Lupus regimen has been widely accepted as remission induction therapy for patients with lupus nephritis. 750 mg of methylprednisolone is given intravenously for three days followed by an oral prednisolone therapy with an initial dose of 0,5 mg/kg/d for four weeks. Then, a dose reduction takes place until a maintenance dose of 5-7,5 mg/day is achieved. In addition to the glucocorticoids, cyclophosphamide is applied at a low-dose regimen including six pulses of 500 mg intravenously every two weeks (81). Instead of cyclophosphamide, mycophenolate mofetil (MMF) can be used. This immunosuppressive drug, inhibiting B and T cell proliferation, has been shown as equal effective as cyclophosphamide in induction therapy (82). Additionally to prednisolone, MMF or azathioprine, acting similar as cyclophosphamide, can be given as maintenance therapy (83). Despite of the effectiveness of these immunosuppressive drugs, complete renal remission, defined as a proteinuria same or lower than 0,5g/day, is only achieved in approximately 20-30% of all patients after 6-12 month after the onset of therapy (84). Furthermore, adverse effects, particularly due to steroids, greatly influence and reduce the quality of life. To counteract this, new targets for further effective treatment options are needed (85).

Indeed, a new drug, called belimumab, has been authorized as add-on treatment in patients with active lupus nephritis by various medical agencies including the European Medical Agency (86). Belimumab is a recombinant monoclonal human IgGγ antibody, that inhibits the B-lymphocyte stimulator (BLyS) leading to a reduced development and survival of B cells. Furie et al. conducted a randomized controlled trial comparing patients with lupus nephritis, which received either belimumab or placebo in addition to the standard therapy (primarily including steroids, cyclophosphamide and MMF). Significantly more patients with belimumab therapy reached the primary efficacy renal response, defined as ratio of urinary protein to creatinine same or lower than 0.7 and an eGFR not worse than 20% of the initial value, than those who received the standard therapy and placebo (87). Another new favourable drug is the calcineurin inhibitor voclosporin, which has been approved by the U.S Food and Drug Administration as add-on therapy for lupus nephritis. The inhibition of the calcium/calmodulin-dependent phosphatase calcineurin results in a reduced cytokine production of T cells, including, among others, tumor necrosis factor alpha (TNF-α), and consequently in an impaired T cell activity. Further monoclonal antibodies, such as binutuzumab and anifrolumab targeting CD20 and IFNs respectively, are currently in Phase

III trials with the aim to develop a wider range of therapeutic opportunities and to reduce or even avoid steroids in the future of the management of lupus nephritis (85).

Currently, the standard regimen in the remission inducing therapy for ANCA-associated vasculitis consists of cyclophosphamide and/or rituximab and high-dose glucocorticoids (79,88,89). A conducted randomized trial (RITUXVAS) showed no inferiority of rituximab comparing to cyclophosphamide for the induction of complete remission within six months although the therapy with CD20 monoclonal antibodies was associated with similar rates of side effects as compared to cyclophosphamide (89). Jayne et al. investigated that cyclophosphamide can be substituted by azathioprine, normally after three months due to a similar rate of relapses between these two immunomodulating drugs. It has been demonstrated that azathioprine shows a considerably lower toxicity compared to cyclophosphamide (47). Consequently, the risk of severe adverse events of cyclophosphamide such as cancer and infertility can be decreased by a shorter duration of drug intake (79).

Due to a possible efficacity of rituximab in the maintenance of remission of ANCA-associated vasculitis (90,91), a nonblinded, randomized, controlled trial (MAINRITSAN) was conducted to compare rituximab infusions and azathioprine in patients after cyclophosphamide-glucocorticoid induction therapy. The study showed a superiority of rituximab compared to cyclophosphamide, at least for patients with proteinase 3-ANCA (PR3-ANCA) (92).

The trial exhibiting the so far largest prospective cohort of patients with relapsing ANCA-associated vasculitis (RITAZERAM) reported that rituximab together with corticosteroids is a potent drug regimen in reinducing remission independent of former therapy (93).

In reference to the therapy regimen of anti-GBM GN, Walsh et. al conducted the PEXIVAS trial to compare the usefulness of plasmapheresis in patients with severe ANCA-associated vasculitis with respect to death or end-stage kidney disease (94). An additional objective of this trial was the investigation of a standardized, effective and relative safe dose regime of glucocorticoids in patients suffering from ANCA-associated vasculitis. Patients were randomly divided into three equal sized groups undergoing either plasma exchange and a standard-dose oral glucocorticoid regimen, plasma exchange and a reduced-dose oral glucocorticoid regimen or no plasma exchange and a standard-dose oral glucocorticoid regimen. The use of plasma exchange did not result in a lower death rate nor in a decreased incidence of end-stage kidney disease among patients with ANCA-associated vasculitis. Furthermore, a reduced-dose regimen of glucocorticoids showed a noninferiority to a

standard-dose regimen with regard to death or end-stage kidney disease. Severe infections occurred more rarely in the reduced-dose group without an increase of the risk of other side effects. These new findings can probably lead to a standardized care regarding the dose regimen of glucocorticoids. Furthermore, avacopan has been studied as an alternative therapy to steroids in ANCA-associated vasculitis. Avacopan inhibits the C5a receptor, a molecule of the alternative pathway of the complement system, responsible for the acute inflammation in the pathogenesis of ANCA-associated vasculitis (Figure 6). In a randomized, controlled trial conducted by Jayne et al., patients suffering from ANCA-associated vasculitis were treated either with oral avacopan at a dose of 30 mg twice a day or with oral prednisolone in a dose reduction schedule. At week 26, avacopan showed an equal effectiveness compared to prednisolone an was even superior to prednisolone at week 52 with respect to remission. Nevertheless, more studies are needed to evaluate the safety profile and the long-term clinical effects of acavopan to be provided as alternative treatment option in ANCA-associated vasculitis (95).

Especially in a high-dose immunosuppressive regime, prophylaxis may be recommended to reduce possible adverse effects. Frequently, prophylactic antimicrobials are used to minimize opportunistic infections, and H2-receptor antagonist or proton pump inhibitors are applied to reduce the risk of peptic ulcers. Further prophylactic measures to be mentioned are the use of bisphosphonates during prolonged corticosteroid therapy to maintain a stable bone density, and the opportunity for sperm or ovum preservation before treatment initiation with gonadotoxic agents such as cyclophosphamide.

Various complications of GN including, among others, hypertension, proteinuria, oedema, and hypercoagulability, are associated with increased morbidity and even mortality and should be actively treated. A successful management may have a positive influence of the disease and may prevent, or at least minimize, the use for immunosuppressive drugs (96).

1.2.2.7 Prognosis

Due to the use of modern immunosuppressive substances, the prognosis of RPGN has improved. When treatment takes place promptly and the kidney still partially functions, an improvement of excretory renal function can be achieved in over 60% of the patients (97).

Furthermore, the patient's outcome strongly depends on serum creatinine at presentation as well as the extent of crescents in the glomeruli found in renal biopsy (74).

Levy et al. demonstrated that patients with anti-GBM GN treated with plasma exchange and immunosuppressive drugs presenting creatinine concentrations less than 500µmol/L (5,7

mg/dL) had 100% patient survival and 95% renal survival at one year. In patients with a creatinine concentration of more than 500 µmol/L (5,7 mg/dL) and with no requirement for dialysis, patient survival was 83% and renal survival 82% at one year (98). Other studies have shown a similar association between elevated serum creatinine and poor prognosis in type 2 and type 3 RPGN (99,100).

Considering renal biopsy, crescents found in more than 80% of glomeruli are associated with a worse outcome in type 2 RPGN (101). Berden et al. analysed 100 renal biopsies from ANCA vasculitis patients and showed that patients with more than 50% of normal glomeruli had a 93% renal survival within five years compared to 76% in those with crescents in more than 50% of all glomeruli (102).

1.3 Experimental crescentic glomerulonephritis: the murine model of Nephrotoxic Serum Nephritis (NTS – model)

1.3.1 Overview of the immune system

The key role of the immune system is the body's host defence against the continuous exposure to other microorganisms. The immune system, a highly interactive network, consists of a variety of effector cells, humoral factors, cytokines and lymphoid organs (47). In general, the immune system can be divided into two main responses, called innate and adaptive immune response. The main difference between these two systems concerns the different generation and expression of the antigen receptors. Whereas the innate immune system carries the antigens on surface proteins with fixed pattern recognition motifs to target common microbial structures, the adaptive immune system generates its antigen receptors by complex DNA rearrangement to detect unique patterns of individual pathogens (103,104). Due to such a mechanism, the adaptive immune response is characterized by a higher sensitivity and specificity. Clonal expansion of adaptive immune cells gives also the possibility to create an immunological memory. Antigen-reactive lymphocytes differentiate into memory cells which will circulate in the blood stream in an inactive state. Once these cells encounter their specific antigen for a second time, they turn into effector cells and trigger an immune response more rapidly in order to prevent an infection (47).

In the following, the principle aspects of innate and adaptive immune system will be discussed in order to gain a better understanding of the immunological mechanisms in the NTS - model knowing well that the processes are much more complex as described below.

1.3.1.1 Innate immune system

The first rapid immune response is performed by the innate immune system which, among others, includes the effector cells neutrophils, monocytes, macrophages, natural killer (NK) cells as well as cytokines and effectors of the complement system (47). The main function of neutrophils is phagocytosis, one of the main mechanisms of the innate immune responses. Thereby, these effector cells, called phagocytes, engulf and subsequently degrade the invaded microorganism by the release of specific enzymes and other antimicrobial substances (105). Macrophages, the mature form of monocytes in the tissue (106), are also able to perform phagocytosis. Nevertheless, the other important function of macrophages is the production of inflammatory mediators, e.g. cytokines of the interleukin-1 (IL-1) family, to activate and recruit other immune cells, especially lymphocytes. This attracting of more specialized immune cells contributes to the induction of adaptive immune responses (Chapter 1.3.1.2) (47). Natural killer (NK) cells have a similar function as cytotoxic T cells (Chapter 1.3.1.2) but they do not have to be activated by the antigen before, which results in a rapid but less specific immune response. NK cells release cytotoxic granules onto the surface of the target cell, inducing cell apoptosis. Simultaneously, the secretion of a high number of cytokines such as INF-γ as well as TNF-α facilitates initiation of adaptive immunity (107). The complement system, assuming a number of important roles in the innate immune system, consists of at least 20 serum glycoproteins. These complement factors C1-C9 are proteolyzed in a cascade leading to their activation and amplification. To date, three pathways of initial complement activation have been discovered, called classical, alternative and lectin pathway resulting all in the activation of C3 component. The further common step is the formation of a membrane attack complex by C5-C9 on the cell surface of the target cell or pathogen to induce cell lysis. Beside inducing cell death, the complement system also has an opsonic function conducted by C3b. C3b binds to the surface of pathogens enabling efficient phagocytosis by macrophages or neutrophils. Furthermore, complement factors, in particular C3a and C5a which possess chemotactic activity, attract more immune cells leading to a greater inflammatory infiltrate in tissue (108).

In addition to neutrophils and macrophages, a third cell type of phagocytes has been identified, called dendritic cell (DC). These cells do also ingest the invaded microbes but, contrary to the other cells, not with the aim of killing them but with the intention of presenting these antigens to T cells in order to activate the adaptive immune response. The DCs act then as link between the innate and adaptive immune response. The innate part of

the immune system lacks of specificity and therefore can occasionally cause damage to healthy tissue (47,108).

1.3.1.2 Adaptive immune system

The adaptive immune response is characterized by an antigen-specific immune response conducted by two major types of lymphocytes called T lymphocytes (T cells) and B lymphocytes (B cells). T and B cells can be distinguished by their highly variable antigen receptors on their cell surface and do perform completely different functions (47).

The activation of T cells takes place in the secondary lymphoid organs, including lymph nodes, spleen, tonsils and mucosa associated lymphoid tissue. Antigen presenting cells such as DCs, B cells and macrophages enter this last-mentioned tissue and try to encounter T cell receptors (TCR), basically composed of α-chains paired to β-chains, that match with the specific antigen they carry. The antigen is expressed on cell surface molecules encoded by highly polymorphic genes of the major histocompatibility complex (MHC) (109). Two classes of this so-called MHC molecules can be distinguished that differ in terms of their structural subunits. Whereas antigens produced within the cells (e.g. viral proteins) are expressed on MHC class I found on the surface of all nucleated cells, exogenous antigens are taken up by endocytosis and expressed on MHC class II molecules that are restricted to antigen presenting cells. The recognition of these MHC molecules by T cells depends on their variable TCRs, and the molecules (CD4 or CD8) they carry on their cell surfaces. $CD8^+$ T cells recognize antigens presented on MHC class I whereas $CD4^+$ T cells interact with MHC class II (108,110). After the interaction with the specific antigen, $CD8^+$ cells differentiate into cytotoxic T cells and are able to kill infected cells carrying the equal antigen (111). T helper (Th) cells characterized by the surface molecule CD4, differentiate into several subsets, including Th1, Th2, Th17 and regulatory T cells (Tregs), to cope a variety of immune functions (112). These subsets differ in terms of their composition of cytokines they secrete as well as the immune cells they target. Th1 cells primarily produce IFN-γ, a pro-inflammatory cytokine leading to an increased expression and antigen presentation of MHC molecules as well as an increased phagocytosis activity by macrophages (113). However, Th2 cells are characterized by the production of IL-4, IL-5, and IL-13 promoting, among others, eosinophil recruitment und mucus secretion by goblet cells, especially found in the respiratory and gastrointestinal tract. Besides being implicated in the immune response against helminths, Th2 cells have shown to play a role in allergic diseases, including asthma and atopic dermatitis (114). Th17 cells particularly induce the recruitment of neutrophils by

the production of IL-17, a potent cytokine family of proinflammatory mediators involved in the host defence against extracellular bacteria and fungi (113). Furthermore, IL-17 was discovered to be overexpressed in various autoimmune diseases, including MS, rheumatoid arthritis (RA), and SLE (115,116). On the contrary, Tregs are a subset of T cells with immunosuppressive function and are mainly characterized by their expression of the transcription factor Forkhead box P3 (Foxp3), a transcription factor crucial for the development and the exercise of regulatory functions of these cells. One mechanism among others of Tregs is the secretion of anti-inflammatory cytokines, including TNF-β and IL-10. TNF-β plays an important role in inhibiting IL-17 production of Th17 cells and increases the expression of Foxp3 in Th cells which results in a larger number of differentiated T Tregs. IL-10 was shown to attenuate the expression of MHC-II molecules. Additionally, the secretion of IL-10 reduces the production of proinflammatory cytokines by macrophages and mast cells. Summarizing, the aim of Tregs is to reduce possible damage to the tissue by the other host immune responses (113).

When T cells first meet their antigen, they highly proliferate to produce enough cells with the specific TCR. Afterwards, they migrate to the site of infection and execute their adequate assigned functions in the host defence. As this process takes a long time, the adaptive immune system is considered as a slow but specific form of immune response (117).

Nevertheless, other subsets of T cells have been discovered to assume immune defence during early infection. Interestingly, these T cells do not interact with MHC molecules and are therefore named “unconventional” or non-MHC-restricted T cells. They bind to non-polymorphic antigen-presenting molecules (e.g. CD1 molecules) and tend to reside in non-lymphoid tissue poised for rapid immune response. Exemplary subsets of this category are CD1d restricted natural killer T (NKT) cells and γδ T cells. CD1d restricted NKT cells in turn can be subdivided into two major types. Type I, also called invariant NKT (iNKT) cell, is mainly characterized by the expression of TCR receptors and surface markers of NK cells such as NK1.1. These cells recognize glycolipids, presented by CD1d, a nonpolymorphic MHC class I-like molecule localized on the surface of antigen presenting cells. One of these glycolipids which activates iNKT cells is α-galactosylceramide, a marine-sponge derived glycolipid which shows high anti-tumor activity (118). iNKT cells constitute a bridge between innate and the adaptive immune system. Besides a rapid secretion of cytokines acting like innate NK cells, iNKT cells express TCRs like conventional adaptive T cells which undergo prior somatic DNA rearrangement. The term “invariant” refers to the

unchangeable α chain in the TCR in iNKT cells, whereas the variety of β-chains is limited but not invariant (118,119).

Analog to the conventional Th cells, iNKT cells can be subdivided into several subsets with different functionalities. Based on cytokine secretion and expression of transcription factors, iNKT cells are classified into iNKT1, iNKT2, iNKT17 and iNKT10 cells which differ strongly from others concerning immune functions (119). On the one hand, they have shown to induce T cell tolerance and to be important for the prevention of autoimmune diseases. Exemplarily, a decreased number of iNKT cells was detected in patients with MS (120). On the other hand, iNKT cells play an active role in the innate immune system by facilitating immune responses against microbes and tumor cells (121).

Whereas iNKT1 cells mainly secrete pro-inflammatory cytokines, including INF-γ, iNKT2 cells mainly execute regulating roles by the production of IL-4. iNKT17 cells are characterized by the secretion of IL-17, a strong pro-inflammatory cytokine as described above (121). A special subset, called iNKT10, has been discovered to maintain macrophage homeostasis in adipose tissue by the secretion of IL-10 (122). Although the cytokine-dependent classification of iNKT cells has become generally accepted, the specific roles of the iNKT cells subsets, especially in autoimmunity, seems to be more complex and not only dependent on their cytokine secretion (121).

In contrast to type I NKT cells, type II NKT cells have shown to have a broader repertoire of TCRs and therefore the possibility to recognize a larger number of different antigens. One ligand interacting with these TCRs is sulfatide. Less elucidated than type I iNKT, type II iNKT cells have been described to have an influence in the downregulation of autoimmunity and tumour immunity. Nowadays, the defence against microbes is assumed secondary (123). In summary, further investigations of NKT cells and their functions in vivo could provide more options for more-effective forms of immunotherapy (118).

γδ T cells are a further subset of unconventional T cells expressing TCRs, composed of a γ-δ-chain, hence the name of this type of cells. Like iNKT cells, they play a role in the innate as well as in the adaptive immune system (124). The innate properties of γδ T cells contain immune responses similar to NK cells, including rapid proliferation and cytokine secretion, in response to tumor cells, inflammation and invading pathogens (125). The capability to perform fast immune reactions is due to their unique tissue distribution. Whereas conventional αβ T cells mainly reside in secondary lymphoid organs, γδ T cells are preferentially located in mucosal and epithelial tissues of peripheral organs. Furthermore, the activation of γδ T cells is made by the direct interaction between the TCRs and their

ligands which are expressed on antigen-presenting cells in a MHC-independent manner (126,127). In humans, a variety of ligands binding to γδ T cells were detected, exemplarily MHC class I-like proteins, including endothelial protein C receptor (ECPR), CD1c and Cd1d (118). Besides the secretion of cytokines such as TNF-α, IFN-γ and IL-17, γδ T cells have shown to have functions of antigen presenting cells by priming conventional αβ T cells at the tumor site and interacting with B cells to facilitate immunoglobulin class switching (128).

B cells are responsible for the humoral immunity in the adaptive immune system. After having recognized a foreign antigen by their B-cell antigen receptor, B cells induce its engulfment and presentation on their cell surface via MHC class II molecules. Under the condition of the pre-activation by Th cells in secondary lymphoid organs, B cell differentiate into plasma cells with the aim to produce specific antibodies to target and bind to this specific epitope on pathogens (129). Due to structural differences, the secreted antibodies by B cells can be principally distinguished into five classes. IgM, secreted as pentamer, is the first class of immunoglobulins produced after activation of B cells. The functions of IgM include, among others, the opsonization of pathogens for the engulfment by phagocytes and the activation of the complement system (130). IgG and IgA are the dominating antibodies in the human body. Whereas IgG is mainly found in blood and extracellular fluid, IgA participates in the mucosal surface defence and is therefore particularly secreted into the intestinal and respiratory tract. Furthermore, IgA is also detected in breast milk. One of the main functions of these two last-mentioned classes of immunoglobulins is to neutralize invading pathogens with the aim to block further infection of the body (131,132). IgE, secreted at very little level into the blood and extracellular fluids, is particularly involved in the immune response against multicellular parasites. Another important function of IgG is to sensitize mast cells, resident innate immune cells mainly found in connective tissue. As a result, mast cells release their granules which are highly rich in various chemical mediators, including histamine, leading exemplarily to allergic diseases such as allergic asthma. The exact functions of IgD, an immunoglobulin class produced and secreted in a very little into the blood serum, remain so far unknown (47,132).

1.3.2 General aspects of NTS

The nephrotoxic serum nephritis (NTS) model was described for the first time by Masugi in the year 1933. His discovery that GN in rodents can be produced by the injection of nephrotoxic antibodies, offers the possibility to investigate the principal

immunopathological processes of experimental CGN and to provide causal explanations for human GN (133).

The general principle of NTS is the intravenous injection of heterologous antibody, raised either in rabbits or sheep, against GBM. The following processes leading to glomerular injury can be divided into two phases. The first, so-called heterologous phase describes the binding of the antibodies to the GBM and, to a lesser extent to tubular basement membrane followed by the activation of the innate immune system and the complement system. These effectors, including among others accumulation of polymorphonuclear granulocytes, deposition of fibrin and necrosis of the capillaries, induce glomerular damage withing 24 hours. In this early reaction, dose-dependent proteinuria can be detected.

The second and usually more severe phase is initiated after three days by the host's adaptive immunity to the heterologous immunoglobulins placed along the GBM. The heterologous antibody acts now as a foreign or "planted" antigen targeted by specific humoral as well as cellular effectors of the adaptive immune system. This autologous phase results in proliferation of renal epithelial cells and infiltration of leukocytes forming so-called crescents within the glomeruli and in nephrotic range-albuminuria (134,135).

NTS has been described as an experimental model for anti-GBM GN for many years (136,137). Nevertheless, the heterologous antibodies aren't specific to α3[IV]NC1 and bind also to other targets in the GBM. Still, some mechanisms in the heterologous phases in the model are comparable to those that occur in human anti-GBM GN, but there's no development of autoimmunity against components of the GBM. The autologous phase better represents the rapidly progressive forms of GN in humans since it's particularly caused by adaptive immune responses that developed a systemic immunity or autoimmunity to antigens in the kidney. Odobasic proposed therefore to describe the first phase of NTS as an immune-complex disease and the autologous phase injury as a "planted antigen glomerulonephritis" (135).

A subcutaneous immunization against IgG of the specimen used in the NTS serum (rabbit or sheep) can be executed 4 to 10 days before NTS application to "accelerate" the model. This allows to induce directly the autologous phase and therefore to facilitate the exploration of particularly T and B cells responses directed against the injected heterologous antibodies (135,137).

1.3.3 Immunological mechanisms of NTS

Innate and adaptive immune mechanisms as well as effectors of the complement system have been detected to play a role in the pathogenesis of NTS (134).

As all experiments have been performed in the accelerated model of NTS with previous immunization, the focus will be particularly on the processes induced by adaptive immune effectors. Theses cellular mechanisms have been graphically highlighted by Kurts et al. (Figure 7) (138).

Several hours after NTS-induction, gamma delta (γδ) T cells, induced by IL-23, start producing IL-17A in the kidney which results in neutrophil recruitment (139). The neutrophils infiltrate the organ immediately and cause renal damage, especially in the glomeruli (134). In addition to this "innate like" γδ cells (139), a T cell specific adaptive immune response, directed against the heterologous antibodies, is initiated by DCs. These renal resident immune cells, physiologically localized in the tubulointerstitium of the kidney, take up, transport and present the antigen to Th cells in the draining lymph nodes (140).

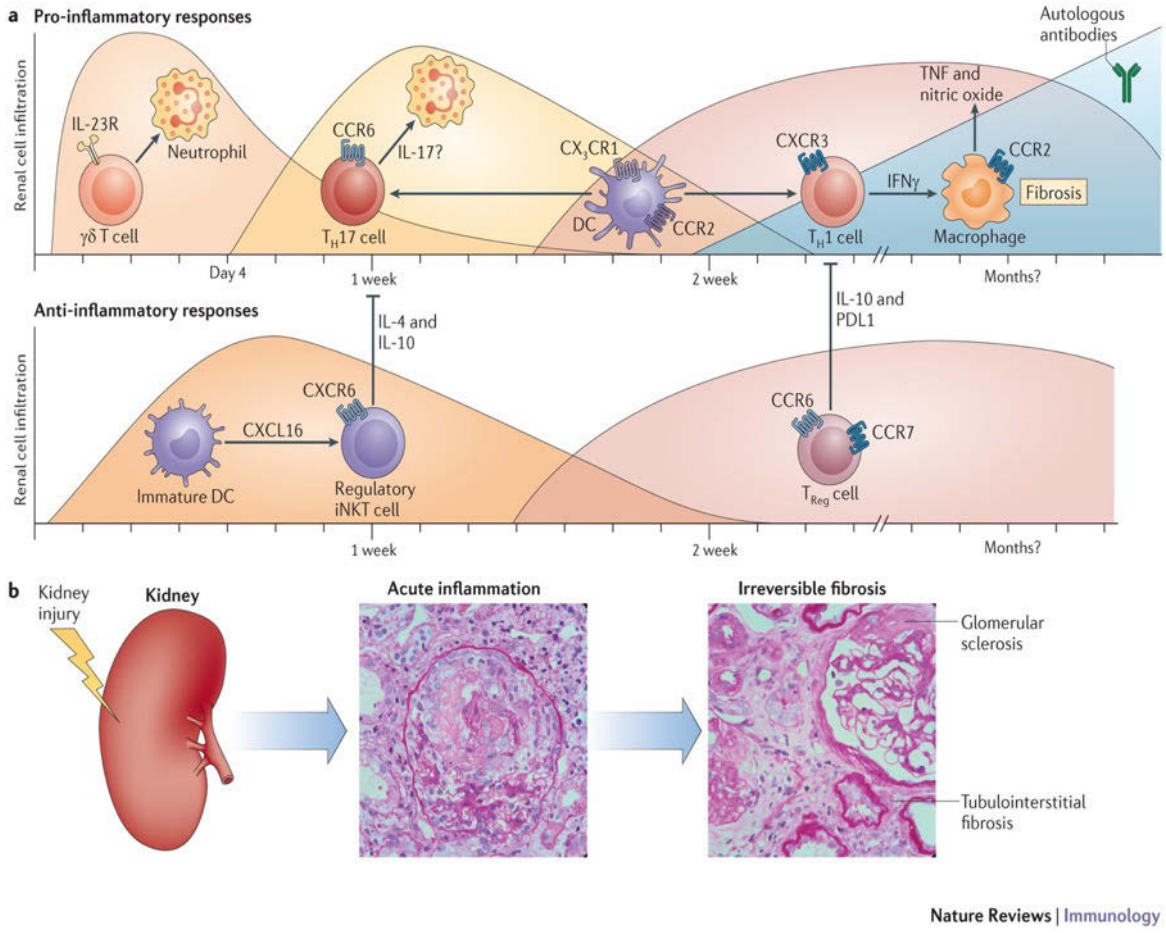

Figure 7: Cellular immune responses in crescentic glomerulonephritis

From: Kurts C, Panzer U, Anders H-J, Rees AJ. The immune system and kidney disease: basic concepts and clinical implications. Nat Rev Immunol. 2013;13(10):738–53 (138).

Th17 cells, expressing CC-chemokine receptor 6 (CCR6), are the first activated Th cells entering the kidney (138,139). IL-17A is the main effector cytokine of Th17 cells, inducing chemokine (C-X-C motif) ligand 5 (CXCL5) expression in the tubular cells of the kidney which in turn recruits neutrophils contributing to more renal damage (141,142). Th17 cells are regulated by iNKT cells expressing the chemokine receptor CXCR6. A study by Riedel et al. suggests that immature DCs, expressing the chemokine ligand CXCL16, act on CXCR6 on the surface of iNKT cells to recruit them to site of injury. By releasing immunomodulatory cytokines such as IL-4, IL 10 and TFGβ, iNKT seem to act as a protective mechanism in NTS (143).

As a next step in the course of NTS, DCs promote Th1 cell activation. Th1 cells recruit more monocytes and fibrocytes into the kidney and produces cytokines such as IFN-γ to enable the conversion of monocytes into macrophages (144,145). These activated macrophages secrete IL-1, which binds to IL-1 receptor on intrinsic renal cells, including endothelial cells, podocytes and mesangial cells, to induce TNF production. These processes lead to an increased infiltration of effector cells and local tissue destruction, forming crescent injury in the Bowman's space (47,144).

Kluger et al. detected an essential role of Tregs, a subpopulation of $CD4^+$ Th cells, mostly defined by the co-expression of CD25 and FoxP3 (146,147), for the counter-regulation of Th17 activity in NTS (148). Thereby, the expression of chemokine receptor CCR6 on the cell surface of Tregs seems to enable the influx of these cells into tissue infiltrated by Th17 cells. In a later phase of disease, Tregs are also able to infiltrate the kidney to attenuate Th1 cell activation by the secretion of IL-10 (138,149). It can be summarized that pro- and anti-inflammatory cells access to the kidney during the progression of NTS. Nevertheless, it has been revealed that secondary lymph organs, particularly draining lymph nodes, are the place where early immune regulation in NTS occur (134). This thesis is supported by a study that transferred $CD4^+CD25^+$ Tregs into mice in the course of NTS model. These mice showed reduced glomerular damage compared to mice that received $CD4^+CD25^-$ Tregs (control group). A further fundamental finding of this study was that Tregs were predominantly found in the lymph node but not in the kidney of the animals (150). Furthermore, Eller et al. investigated the potential role of chemokine receptor CCR7 regarding the migration of Tregs in NTS (151). This chemokine receptor is not only expressed on Tregs but also on DCs and $CD4^+$ T cells and interacts with two ligands, named CCL19 and CCL21. This interaction of ligand and chemokine receptor leads to an enhanced migration of these DCs and $CD4^+$ T cells into T cell regions in lymph nodes, where antigen presentation to T cells and

differentiation into effector T cells takes place (152). Eller et al. reported that CCR7 knock-out mice showed a highly increased number of infiltrating inflammatory cells and Tregs in the kidney and a more severe glomerular damage compared to wild-type mice. These Tregs found in the kidneys of CCR7 knock-out mice were unable to fulfil their role as down-regulator of the proinflammatory activity in NTS. Consequently, it has to be assumed that CCR7 is needed for the Treg mediated inhibition of disease progression, which seems to take place in lymph nodes (151).

The function of $CD8^+$ T cells in crescentic forms of GN has been studied, among others, by Tipping et al. in the year 1998. He showed that CD4 knock-out mice developed mild crescentic GN seven days after the injection of sheep anti-mouse GBM globulin. Conversely, CD8-deficient mice developed severe glomerular injury with ascites and oedema. These studies supposed that crescentic formation within the glomeruli happens in a CD4-dependent but CD8-independent way (153). Nevertheless, the role of $CD8^+$ T cells in mice models of crescentic GN remains controversial until today. Since $CD8^+$ T cells have been detected in periglomerular infiltrates, among others, in lupus nephritis, it seems nevertheless possible that T cell-mediated cytotoxicity is part of the effector mechanisms in NTS (154). This hypothesis is supported by a study of Heymann et al., which showed a pronounced periglomerular mononuclear infiltration in transgenic mice as a result after the injection of $CD8^+$ T cells and $CD4^+$ Th cells, specifically directed against a specific glomerular structure (155). Furthermore, these findings show the importance of the mature DCs cross-presenting glomerular antigen to the $CD8^+$ T cells in renal lymph nodes. According to Heymann, activated $CD8^+$ T cells enter the kidney and liberate more glomerular antigen which in turn increase the cross-presentation in renal lymph nodes. DCs in the tubulointerstitium also take up these molecules, presenting them to specific Th cells such as Th17 and Th1 leading to a constant periglomerular infiltration of effectors cells, production of proinflammatory cytokines and chemokines and thereby to a progression of the renal injury.

In summary, the severeness of NTS, and thus whether the kidney injury resolves or progresses to fibrosis and sclerosis, does not only depend on pro-inflammatory, but also on anti-inflammatory T cells (138).

As mentioned before, the complement system also contributes to the pathogenesis of NTS, particularly in the “accelerated” model of NTS (134). The classical pathway of the complement is activated by IgG and IgM immune complexes deposited in the GBM (156). Several studies have shown a beneficial effect in NTS by the inhibition of complement pathways (134,157–159). However, deficiencies of C1q or C4, a predisposition for the

development of SLE (Chapter 1.2.2.4), result in severe glomerular injury in NTS, probably due to an incorrect clearance of immune complexes or apoptotic cells in the absence of these complement components (160).

1.4 Sphingosine 1-Phosphate

Gosh et al. were the first to show that intracellular conversion of sphingosine to sphingosine 1-phosphate (S1P), both belonging to the class of sphingolipids, results in an increased calcium release from a calcium pool, including 1,4,5-triphosphate-senstitive calcium from the endoplasmatic reticulum (161). Two sphingosine kinases (SK), named SK-1 and SK-2, that catalyse the phosphorylation of sphingosine, have been identified until today. These subtypes and their detected splice variants are differently expressed in tissue and don't exhibit equal biochemical properties, for example their substrate specificity. These findings suggest that the cellular functions of S1P may be different depending on its generation by either SK-1 or SK-2 (162,163). The S1P molecule shows signalling properties similar to those of chemokines and acts as an extracellular ligand on G-protein coupled receptors on the cell surface. Five subtypes, called S1PR1 – 5, have been identified until today and each of them provokes diverse cellular responses depending on the cell type.

Because of the detection of SK's as well as S1PRs in renal cells, much time and effort has been spent since then to elucidate the physiological and pathophysiological functions of S1P in the kidney. S1P and its receptors may be new targets for treatment of several kidney diseases, including GN (162).

The main functions of S1P and S1PRs which have been identified in the kidney until today will be summarized with a special focus on their roles in the pathogenesis of GN.

Cellular responses triggered by S1P can have an impact on proliferation, cell survival or migration depending on the cell type. In particular, MC cell proliferation in the glomeruli seems to be positively influenced by S1P. In many forms of GNs, MCs show an increased proliferation as well as production of extracellular matrix component and inflammatory mediators (162). Because of these findings, S1P as a potent growth factor, has become a possible new target in the treatment of glomerular diseases (164).

Referring to cell survival, Hofmann et al. have discovered that SK-1 and SK-2 act differently in mesangial cells. The function of SK-1 seems to be the inhibition of apoptosis, whereas SK-2 acts as a pro-apoptotic enzyme (165). Furthermore, it was shown that in renal MC cultures, SK-1 can be activated by extracellular S1P and other extracellular nucleotides, including adenosine triphosphate (ATP) and uridine triphosphate (UTP), and afterwards

contribute to MC migration, a characteristic process especially found in mesangioproliferative GN (162,166).

S1P plays also a crucial role in immune cell trafficking. Chemical modification of ISP-1, a component isolated from the *Isaria sinclairii*, a fungus particularly found in Asia, resulted in a potent new immunosuppressive drug, named FTY720 (167). It was reported that FTY720, following a prior phosphorylation by SK's, acts as a potent agonist on S1PRs 1,3,4 and 5 in mice and shows an inhibitory effect on T cell emigration from the thymus to the periphery (168,169). At that time, the exact role of S1PRs in immune cell trafficking remained still unclear. Eventually, Matloubian et al. showed in adoptive cell transfer experiments that the expression of S1P1 on the surface of T and B cells is required for the egress from the secondary lymphoid organs back to the circulation. During T cell activation in lymphoid tissue, S1P1 is downregulated to retain the immune cells in the tissue. Once T cell activation recedes, S1P1 expression increases, allowing T cells to migrate along a S1P concentration gradient to the periphery (170). At a later time, Gräler et al. described FTY720 not as a classical agonist but as a potent S1P1, 2 and 5 receptor inhibitor, that causes their internalization and intracellular degradation, reducing the circulating numbers of lymphocytes (171). On the basis of its main effect to inhibit lymphocyte's migration to the periphery, FTY720, also known as fingolimod (Gilenya®), can be used as a potential drug for the treatment of diseases with altered adaptive immune responses. In 2011, it has been approved for oral treatment for relapse-remitting multiple sclerosis (RRMS) in the European Union (EU) (172). As fingolimod acts on several S1PRs and therefore lacks specificity, novel compounds similar to fingolimod have been developed with the aim to enhance efficacy and tolerability (173). One next-generation S1PR modulator, selective for S1P1 and S1P5, called BAF-312 (siponimod, Mayzent®), has been approved among others in the EU and in the USA for the treatment of secondary progressive multiple sclerosis (SPMS) (174). Some studies evaluated the effect of FTY720 in experimental anti-Thy.1.1-induced GN, a model for progressive mesangioproliferative GN. They could show a negative influence on the progression of renal injury by treating rats with this functional antagonist of S1P. The results showed decreased lymphocyte infiltration as well as reduced proteinuria, tubulointerstitial matrix expansion, transforming growth factor beta 1 (TGF-β1) and fibronectin expression (162,175,176).

Furthermore, Sui et al. showed in a mouse anti-GBM model a beneficial effect of FTY720 against glomerular damage. Mice treated with FTY720 for 14 days showed reduced proteinuria, serum creatinine, crescent formation within the glomeruli and serum IgG level.

Lower expression of S1PRs 1,2 and 5 in the spleen and a decreased production of cytokines of Th1 cells in the kidney could be detected, although the exact mechanism remains still unknown (177). Regarding the effect of FTY720 on Tregs, Wolf et al. showed its potential inhibitory function by trapping Tregs, mainly expressing S1P1 onto their cell surface, in inflammatory secondary lymphoid organs. Simultaneously, FTY720 seems to impair the immunosuppressive activity of Tregs by the inhibition of Treg expansion (178).

This diploma thesis places special focus on the S1P5, whose function in the kidney and in the pathogenesis of GN remains still unknown. The so far last identified S1PR is primarily expressed on oligodendrocytes and the endothelium in the central nervous systems (CNS) (179,180). In addition, expression of S1P5 was also found on NK cells and is required for the NK cell migration to inflamed organs (181). The function of S1P5 in renal diseases remain still unknown. In cell culture trials, Wünsche et al. revealed that the expression of S1P5 in MCs is induced by the tissue growth factor TGF-β2, contributing to the formation of renal fibrosis. Simultaneously, depletion of S1P5 seems to have an antifibrotic effect and inhibits the TGF-β2-mediated expression of the CTGF (182).

Within the NTS model, preliminary experiments of the working group of Kathrin Eller from the Department of Nephrology at the Medical University of Graz with the collaboration of Alexander Koch of the pharmazentrum frankfurt/ZAFES at the Johann Wolfgang Goethe-University Frankfurt showed in an 80-fold increase of mRNA expression levels of S1P5 in the kidney of NTS injected-mice compared to the healthy control group (day 7). Interestingly, the expression regresses on day 14. Furthermore, when comparing S1P5-deficient (knock-out) mice and wild-type mice, a massive decrease in albuminuria in S1P5-deficient mice in the NTS model was found. These findings show impressively that S1P5 plays a role in the NTS model and thus, quite likely in human RPGN. A greater understanding and knowledge of its function could lead to the development of selective S1P5 modulators as further therapeutic options in the treatment of RPGN. This is highly relevant because untreated RPGN can lead to end-stage renal disease and current treatment possibilities are frequently accompanied by severe adverse effects (Chapter 1.2.2.6).

2 Material and Methods

2.1 Ethics statements

All animal experiments were approved by the Austrian National Animal Experiment Ethics Committee of the Bundesministerium für Wissenschaft und Forschung (BMWF-66.010/0057-WF/V/3b/2014). All procedures related with animal experimentations were strictly performed according to the Austrian law (Tierversuchsgesetz TVG 2012, BGBl. I Nr. 114/2012).

2.2 Induction of NTS and treatment

For conducting the study, mice from the inbred strain C57BL/6J (Charles River Laboratories, Sulzfeld, Germany) were maintained in a pathogen-free facility at the Center for Medical Research (Medical University of Graz, Austria). The regular, grain based diet for feeding the mice was obtained by Ssniff Spezialdiäten GmbH (Soest, Germany). The design of sniff® diets as well as the construction of the cages allowed the mice to have access to food and water ad libitum.

15 mice male mice (littermates) at the age of 8 to 12 weeks were randomly and equally categorized into three groups: a vehicle (negative control) group, a BAF-312 (positive control) group and a group treated with a selective agonist of S1P5 named A-971432 (183). Before the application of NTS (Chapter 1.3), the mice were immunized. Therefore, a solution was prepared containing 178,5 µL of 2 mg/mL rabbit IgG (Jackson ImmunoResearch Laboratories, West Grove, PA, USA), 1 mL of incomplete Freund´s adjuvant (Sigma-Aldrich, St. Louis, MO, USA), 10 mg of nonviable Mycobacterium tuberculosis H37a (Difco Laboratories, Detroit, MI, USA) and 821,5 µL of phosphate-buffered saline (PBS, 6,71 g NaCl, 0,4 g KH_2PO_4, 1,42 g Na_2HPO_4 in 1 L of distilled water). The subcutaneous immunization of 100 µL for each mouse was administered into the right food. On the same day, the first daily intraperitoneal injection of A-971432 (Tocris Bioscience, Bristol, UK), BAF-312 (Selleck Chemicals Inc., Houston, TX, USA) and the vehicle took place for the three respective groups. The doses were 0,1 mg/kg bodyweight per day for A-971432 (183) and 3 mg/kg bodyweight per day for BAF-312 (184,185). The daily treatment occurred at the same time of day and the injection side was always situated at the left lower quadrant of the abdomen. It was important to hold the mice in head down position to avoid any damage to internal organs. Three days after immunization, the mice were injected intravenously with 0,1 mL of the heat-inactivated NTS into the tail vein. The daily injections of the vehicle-

solution, BAF-312 and A-971432 ended at day 9 after NTS-induction and urine samples were collected at day 0, 7, and 9.

2.3 The method of sampling

On the last day of the experiment (day 9), a blood sample of each mouse was collected in micro tubes. This blood was needed to obtain blood serum afterwards (Chapter 2.5). Subsequently, the mice underwent terminal anaesthesia and cervical dislocation. With this method, the neck was hold with two or three fingers applying sufficient pressure on it and by that the spinal column was separated from the skull and brain. After the fixation of the mice in a dorsal position, a vertical incision on the midline of the abdomen as well as a transversal incision in the inguinal region was made and the abdominal cavity was exposed. First, the inguinal lymph node on the immunization side and the paraaortic lymph node were carefully dissected, followed by the preparation of the spleen and the two kidneys. At last, the left femur was removed. The two ends of the bone were cut off until the bone marrow could be detected. To extract and stabilize the bone marrow, 1 mL of RNAlater™ Stabilization Solution (Thermo Fisher Scientific Inc., Carlsbad, CA, USA) was drawn into a syringe. A needle was attached to the syringe and positioned at one end of the femur. The inner of the bone was rinsed with RNAlater ™ to extract the bone marrow. Last-mentioned along with the RNAlater ™ was stored in a micro tube.

The weight of the inguinal lymph node was well noted for subsequent flow cytometry evaluation. Then, the inguinal lymph node was divided into two halves. One of them was weighted and placed in a well of a Falcon® 12-well plate (BD Biosciences, San José, CA, USA) filled with PBS. The other half as well as the entire paraaortic lymph node were stored separately in a RNA tube and snap-frozen in liquid nitrogen. The spleen was weighted entirely, a third was cut off, weighted separately and also brought in a well of a Falcon® 12-well plate. The rest of the spleen was snap-frozen in liquid nitrogen. One kidney was divided into two halves fixing one part in formalin for the PAS-staining (Chapter 2.6) and preserved in storage at minus four degrees Celsius. The other part was snap-frozen with Tissue-Trek® OCT™ Compound (Sekura Finetek Europe B.V., Alphen aan den Rijn Netherlands) for the immunohistochemical staining (Chapter 2.7) and stored at minus 20 degrees Celsius. The other kidney was put in a RNA-tube and snap-frozen with liquid nitrogen.

2.4 Determination of albumin-to-creatinine ratio

The level of albumin in the urine has been accepted as an important marker for renal disease and is directly related to its progression (7). Albumin with a molecular weight of approximately 65kDa (186) is the most abundant plasma protein. A number of various functions has been described, inter alia, the maintenance of the oncotic pressure and blood volume, acid/base buffer functions and the transport of several substances (187). Physiologically, very little albumin can be detected in the urine. This is largely because of the highly selective glomerular filtration barrier, whereby mostly albumin and larger molecules are retained. The negative charge of both albumin and the GBM also interferes the passage of albumin into Bowman's space. Albumin that does leak the glomerular filtration barrier is then resorbed in the proximal tubule by endocytosis (187,188).

Urinary albumin excretion shows a high intraindividual variability depending on the individual's fluid intake and physical activity. If the urine is concentrated, for example after physical activity, increased protein concentration can be falsely interpreted. On the other hand, the albumin secretion can be underestimated in a strongly diluted urine. To account for these fluctuations, a 24-hours urine collection has been considered the "gold standard" to measure albuminuria for a long time. Nevertheless, in daily clinical practice collecting urine during a day is connected with high efforts and, in context of experiments with mice, not feasible. To replace this method, measures in a spot urine and results given as albumin-to-creatinine ratio have been proposed. Creatinine (Chapter 1.1), a product from muscle and protein metabolism, is assumed to be secreted at a constant rate in the urine and can be used to normalize the amount of albumin. Dividing albumin by the creatinine concentration leads to a reduction of the intraindividual variation in albumin excretion (189,190).

2.4.1 Albumin-ELISA

For the quantitative detection of albumin levels in mouse urine, a sandwich enzyme-linked immunosorbent assay (ELISA) was used. The basic principle of a sandwich ELISA is the detection of an analyte in a liquid sample by using specific antibodies directed against the antigen to be tested.

All steps have been performed strictly according to the protocol. Firstly, goat anti-mouse albumin (Bethyl A90-134A-5, Bethyl Lab Inc., Montgomery, TX, USA) in a concentration of 0,1 mg/mL was diluted with a compound of sodium carbonate and sodium hydrogen carbonate (1,59 g Na_2CO_3, 2,93 g $NaHCO_3$ in 1 L of distilled water, pH 9,5). A 96-well

microplate (Nunc Edge, Thermo Scientific, Langenselbold, Germany) was then coated with 100 µL per well of the prepared solution and incubated overnight at four degrees Celsius.
The next morning, the microplate was washed three times with 0.05% PBS-Tween buffer (6,71 g NaCl, 0,4 g KH_2PO_4, 1,42 g Na_2HPO_4, 500 µL Tween 20/Polysorbat 20 [Sigma-Aldrich] in 1 L of distilled water, pH 7,4).
125 µL of the blocking solution, containing bovine serum albumin (BSA) with a concentration of 0,5% (SERVA Elektrophoresis GmbH) and PBS-Tween, was added to each well and incubated for 30 minutes at room temperature.
Dilution series of the samples (mouse-albumin, 1 µL/mL, 0,3 µL/mL, 0,1 µL/mL, 0,03 µL/mL, 0,01 µL/mL, 0,001 µL/mL, 0,0 µL/mL) as well as of a albumin standard solution were prepared using PBS-Tween as dilution solution. 100 µL of each dilution was used in triplicates and incubated for two hours at room temperature.
After washing three times again, a goat anti-mouse albumin antibody (Bethyl A90-134P-7, Bethyl Lab Inc.) at a concentration of 0,02 µg/mL was diluted in PBS-Tween. 100 µL of the solution was then added to each well.
This detection antibody is conjugated with horseradish peroxidase (HRP) required to convert a substrate consisting of tetramethylbenzene (TMB) buffer and hydrogen peroxide. After two hours of incubation at room temperature and another three washing steps, this substrate was added with a quantity of 100 µL per well.
After an incubation period of ten minutes in the dark, the enzyme reaction was stopped with 50 µL of H_2SO_4 per well and the optical density (OD) was measured by means of a photometer (FLUOstar Omega, BMG LABTECH GmbH, Ortenberg, Germany) at wavelength of 450 nm.
The calculation of the albumin concentration was done using regression analysis. With the help of the known standard dilution series, a standard curve (4-Patameter fit based on Blank corrected) was created. The logarithm of the concentration was shown on the x-axis and the linear OD on the y-axis. The albumin concentration could then be read in the linear range of the resulting sigmoid curve. The exact values in µg/mL were calculated with the help of the software of the photometer.

2.4.2 Creatinine assay

Urinary creatinine was evaluated using a picric acid-based kit (Sigma-Aldrich). In alkaline solution, picric acid and creatinine form a reddish-orange complex that can be measured using photometry. All steps have been performed strictly according to the protocol.

As a first step, the alkaline picrate solution was prepared according to the protocol. The urine samples were diluted 1:10 with distilled water. Blank solution (distilled water), standard solution included in the kit, and the samples were applied with a quantity of 10 µL per well in triplicate to a 96-well microplate (Greiner Bio-One International AG, Kremsmünster, Österreich). 176 µL per well of the prepared solution was then added to the microplate. After an incubation period of 12 minutes at room temperature, the OD was read photometrically (FLUOstar Omega, BMG LABTECH GmbH, Ortenberg, Germany) at wavelength of 490 nm. 6 µL per well of acid reagent, comprised in the kit, was subsequently added to each well and the microplate was incubated for five minutes at room temperature. Another reading at wavelength 490 nm was done. The creatinine concentration was then calculated in accordance with the following formula:

$$Creatinine = (sample_{initial} - standard_{final}) \cdot 3$$

Equation 5: Calculation of creatinine concentration in [mg/dL]

2.5 Titre determination of anti-rabbit-IgG in mouse serum

For the relative quantification of circulating autologous antibodies against induced heterologous rabbit anti-mouse antibodies in the mouse serum (Chapter 1.3), a method similar to the albumin-ELISA was used.

A coating solution containing sodium carbonate and sodium hydrogen carbonate (1,59 g Na_2CO_3, 2,93 g $NaHCO_3$ in 1 L of distilled water, pH 9,5) as well as 100 µL/mL rabbit IgG (Jackson ImmunoResearch Laboratoris Inc.) was prepared. 100 µL per well was added to a 96-well-microplate (Nunc Edge, Thermo Scientific, Langenselbold, Germany) and incubated over night at four degrees Celsius.

The next morning, 125 µL of the blocking solution, containing BSA standard solution with a concentration of 1% (SERVA Elektrophoresis GmbH) and PBS-Tween buffer was added to each well and incubated for 30 minutes at room temperature. Before and after blocking, the microplate was washed three times with 0.05% PBS-Tween buffer.

For the extraction of serum, blood samples from mice were centrifugated and the supernatant was isolated. Dilution series of the samples (mouse serum, 1:1600, 1:32000, 1:64000, 1:12800) were prepared. 0,05% PBS-Tween was used as diluent. 100 µL per well of each dilution was used in duplicates which was then incubated for two hours at room temperature. After a further three washing steps, 100 µL per well of HRP-conjugated goat anti-mouse IgG (P0447, Dako Österreich GmbH, Vienna, Austria), diluted in 0,05% PBS-Tween buffer

in a 1:5000 ratio, was added to the microplate and again incubated for two hours at room temperature.

As in the case of the albumin-ELISA, a solution consisting of TMB buffer and hydrogen peroxide was used as substrate, filled in the wells of the microplate (100µL/well) and incubated in the dark for five to ten minutes. The enzyme reaction was stopped with 50 µL of H_2SO_4 per well and the OD was measured by means of a photometer (FLUOstar Omega, BMG LABTECH GmbH, Ortenberg, Germany) at wavelength of 450 nm. The quantification of anti-rabbit-IgG was not evaluated by the use of a standard curve as in the case of the albumin concentrations in the urine (see above), but by the detection of the four titre levels.

2.6 Periodic acid-Schiff (PAS) staining

Periodic acid-Schiff (PAS) is a histochemical staining used to detect carbohydrates such as polysaccharides, glycoproteins, glycolipids and mucins. Periodic acid reacts with 1,2 glycol linkage of carbohydrates and forms aldehydes. These aldehydes are then coloured with Schiff's reagent, based on a sulfurous acid and an aqueous solution of basic fuchsin, which turns into a red-violet colour when it's bound to an aldehyde. This staining method can be useful to represent PAS-positive material in the glomerular basement membrane (GBM) and subsequently to evaluate the extent of glomerulosclerosis (191–193).

The kidneys of the mice, fixed in formalin (Chapter 2.3), were firstly dehydrated through a series of graded ethanol baths, and then embedded in paraffin. With the help of a rotational microtome, cut cross-sections of the tissue were performed at a thickness of 4 µm and placed on a microscope slide.

For the PAS staining, all steps have been performed strictly under the extractor hood and according to the protocol. The first step included the deparaffination and rehydration with xylol and a graded ethanol series. After rinsing in distilled water, the cross-sections were placed into periodic acid (Merck KGaA, Darmstadt, Germany) for ten minutes. This step was followed by rinsing the slides with running water for three minutes and subsequently with distilled water. Schiff's reagent (Merck KGaA) was then added to bind to the aldehyde groups and to form red-violet complexes. After a further washing step with running water and distilled water, the cross-sections were counterstained with haematoxylin (Gill III, Sigma-Aldrich) followed by rinsing with running water for three minutes. A renewed dehydration with a graded ethanol series and xylol was executed. The microscope slides were left to air dry and then equipped with the mounting medium Roti® Histokitt (Carl Roth, Karlsruhe, Germany) and a cover glass.

The evaluation was conducted using light microscopy. The test person was blinded and therefore couldn't assign the microscope slide to the respective experimental group. A following semiquantitative scoring system was applied to assess a minimum of 50 glomeruli in each cross-section:

G0 = the glomerulus doesn't show any PAS-positive material / G1 = up to one third of the glomerulus shows PAS-positive material / G2 = one third up to a maximum of two thirds of the glomerulus shows PAS-positive material / G3 = more than 2 third of the glomerulus shows PAS-positive material

The PAS-score was then calculated by the following formula:

$$\frac{0 * number\ of G0 + 1 * number\ of\ G1 + number\ of\ G2 + number\ of\ G3}{sum\ of\ G0 + G1 + G2 + G3}$$

Equation 6: Calculation of PAS-score

A mean value of the PAS-score was evaluated for each experimental group. Furthermore, tubular casts, reflecting damage to the renal tubules, have been evaluated by counting their number in six high power fields (HPF, 400x magnification) for each sample.

2.7 Immunohistochemistry

A method for detecting a protein in tissue sections is immunohistochemistry, whereby the specific antibody (direct method) or the secondary antibody (indirect method) is bound to an enzyme that transforms an uncoloured substrate into a coloured reaction product. The localization and quantity of stained deposits can then be observed under a light microscope. This approach of detecting bound antibody is comparable to ELISA (Chapter 2.4.1) and often uses the same coupled enzyme, such as HRP or alkaline phosphate. The difference in detection being primarily that in immunohistochemistry the coloured products aren't insoluble and precipitate at the site where they are formed (47,194).

Immunohistochemical staining is a useful tool to detect cluster of differentiation (CD) antigens, molecules found on the surface of leukocytes and other cells relevant for the immune system (195), allowing to distinguish between the different immune cells. Ly6G, a marker for neutrophils, can also be identified using this method.

2.7.1 CD4

CD4, a single chain protein composed of four Ig-like domains, is mostly expressed by helper T cells. It can also be found in thymocyte subsets, in regulatory T cells, some NKT cells and some monocytes and macrophages. During antigen recognition, CD4 is associated to the T-

cell receptor and binds to MHC class II to enhance sensitivity to antigen. CD4 immunohistochemical staining is primarily designed for the detection of Th cells in tissue sections (47).

2.7.2 CD8

CD8 is a disulfide-linked dimer of two different chains, each including a single Ig-like domain linked to the membrane. The expression of CD8 is mostly found in cytotoxic T cells. Like CD4, CD8 is acting as a co-receptor for T cell receptor but binds to MHC class I increasing the sensitivity of T cells to the antigen. It is used for the detection of cytotoxic T cells in the tissue (47).

2.7.3 CD68

CD68 is highly expressed by monocytes and macrophages (196). This glycosylated transmembrane protein is a member of the lysosome-associated membrane glycoprotein (LAMP) family and primarily localized in lysosomes, endosomes and with a smaller proportion to the cell surface (197). The function of CD68 remains still unknown but studies have shown that it could play a role in cell adhesion and internalization of bound ligands at the cell surface (198). CD68-antibody-staining is used for the assessment of macrophages.

2.7.4 Ly6G

Ly6G belongs to the Ly6 family proteins which all share a conserved motif, known as the LU domain, and most of all are bound to the cell surface through a C-terminal glycosylphosphatidylinositol (GPI) anchor (199). Although the physiological function remains still unclear, Ly6G plays an important role as a specific marker that distinguishes neutrophils from other leukocytes and as a target for antibody-mediated depletion of neutrophils (200). Ly6G is expressed only in mice, but a structurally related family member, CD177, has been detected that is expressed on human neutrophils (201).

2.7.5 Procedure

Frozen kidney sections (Chapter 2.3) were processed at a thickness of 4 µm with a cryostat-microtome. The tissue sections were then picked up on a microscope slide.

For the immunohistochemical staining, all steps have been performed strictly according to the protocol. First, the tissue sections were air dried at room temperature for 30 minutes and subsequently fixed with acetone (Merck KGaA) at four degrees Celsius for eight minutes. A

circle with a fat pencil (Dako Pen, Dako Österreich GmbH) was drawn around the tissue sections to create a hydrophobic barrier and keep all staining substances localized on the tissue sections.

To prevent non-specific binding, a blocking solution containing 20% of fetal calf serum (FCS, Sigma-Aldrich), 10% of goat serum (Sigma-Aldrich Chemie, GmbH) and 70% of PBS was prepared. Avidin included in the Avidin/Biotin Blocking Kit (Vector Laboratories Inc., Burlingame, CA, USA) was added additionally. It's a tetrameric biotin-binding glycoprotein and found in the egg white of birds (202,203). The aim of the blocking kit is to bind to all endogenous biotin and avidin binding sites present in tissues. 200 µL of the blocking solution was applied to each tissue section which were subsequently incubated for 20 minutes in a moist chamber.

After washing two times for one minute with PBS, tissue sections were plunged into 2% gelatine solution (0,8 g gelatine, 100 mL distilled water and 300 mL PBS) for two minutes. This step was followed by the application of rat-derived primary antibodies directed against the antigen of interest. Adapted to the respective staining, antibodies for CD4 (clone YTS191.1; Serotec, Oxford, UK), CD8 (clone KT15, Serotec), CD68 (clone FA-11, Serotec) or Ly6G (clone 1A8, Abcam, Cambridge, UK) were used. A solution of 2 µL/mL of primary antibody (diluted in PBS) and 4 drops/mL of biotin from the Avidin/Biotin Blocking Kit (Vector Laboratories Inc.) were prepared. Each kidney section was then stained with 200 µL of the mixture and incubated for two hours in a moisture chamber. After the incubation, another washing step with PBS was done.

A biotin-conjugated goat anti-rat IgG (secondary antibody) with a concentration of 5 µL/mL was applied to the kidney sections (200 µL/section) and incubated for 45 minutes in a moist chamber. After incubation with the secondary antibody, all sections were washed again with PBS for three times.

To achieve greater signal amplification, high affinity molecules such as avidin and biotin are utilized. Avidin binds almost irreversibly to biotin. By labelling secondary antibodies with biotin (see above) as well as HRP with biotin, these two compounds can then be linked by avidin irreversibly (204). For this procedure, an avidin-biotin complex (ABC) from a standard kit (Vectastain, Elite ABC HRP Kit, Vector, Laboratories, Burlingame, CA, USA) was created strictly according to the protocol and applied to the kidney sections (200µL/section). The incubation period for the ABC was 30 minutes followed by a washing step with PBS.

As mentioned at the beginning of this subchapter, biotinylated-HRP converts a substrate to a colour signal. This chromogenic solution consisting of 0,2 mL of 3-amino-9-ethylcarbazole (AEC [Sigma-Aldrich], six tablets to be dissolved in 30 mL of n,n-dimethylformamide), 4 mL of 0,1 M acetate buffer (300 mL of 0,2 M sodium-acetate and 100 mL of acetic acid in 400 mL of distilled water) and 2 µL of hydrogen peroxide (H_2O_2), was prepared under the extractor hood in the dark and subsequently added to the kidney sections. After detecting colour change under the microscope, the sections were washed with distilled water and then counterstained with haematoxylin (Gill III, Sigma-Aldrich).

For the quantitative evaluation of $CD4^+$, $CD8^+$ and $Ly6G^+$ cells, stained cells were counted in six HPF (400x magnification) in renal cortex and medulla. A mean value of the six HPFs was calculated for each sample.

$CD68^+$ cells were assessed in four low power fields (LPF, 200x magnification) using the following semiquantitative scoring system:

0 = 0-4 cells stained positive / 1 = 5-10 cells stained positive / 2 = 11-50 cells stained positive / 3 = 51-200 cells stained positive / 4 = > 200 cells stained positive

A mean value of the four LPFs was calculated for each sample.

2.8 Establishment of CD1d-tetramer staining and confocal analysis

With the aim of evaluating NKT cells in spleen, we established a CD1d specific tetramer staining, a method slightly similar to the immunohistochemical staining mentioned above. Generally, a tetramer assay is used to identify antigen-specific T cells by making up tetrameric proteins formed by four MHC complexes. Each of these MHC molecules is linked to an antigen that matches specifically the T cells to be quantified. Furthermore, the tetramers are labelled by a fluorophore such as phycoerythrin (PE) admitting the analyzation of the stained cells by the use of confocal laser scanning microscopy (CLSM). It has been shown that the affinity between a peptide and the tetramer is highly increased compared to the binding of only one MHC-molecule to the peptide. Therefore, tetramers enable and facilitate the identification of T cells (47).

In our particular procedure, CD1d, a member of the CD1 family of MHC class I-like molecules, expressed on antigen-presenting cells in mice is used to form these tetramers. Studies have demonstrated that CD1d molecules primarily bind specific glycolipids, such as α-galactosylceramide. Therefore, PBS-57, an analogue of α-galactosylceramide has been developed by Liu et al. aiming to function as the specific antigen (205).

Before staining of all available samples, an adequate dilution factor of the tetramer reagents had to be assessed. Therefore, several test samples were stained with different dilutions (1:50, 1:100, 1:1200 and 1:500). After evaluating the slides under confocal laser scanning microscopy (CLSM), the least diluted samples (1:50) had showed the most suitable signal for the quantification of the NKT cells.

At the beginning of the procedure, a part of the spleen of each sample was embedded in Tissue-Trek® OCT™ Compound (Sekura Finetek Europe B.V., Alphen aan den Rijn Netherlands) and subsequently stored at minus 20 degrees. The following first steps were performed equally to those in immunohistochemistry (Chapter 2.7). Frozen spleen sections have been cut at a thickness of four µm and placed on a microscope slide. The slides were air dried at room temperature for 30 minutes and acetone (Merck KGaA) was applied on the samples for eight minutes. Subsequently, a rehydration in PBS for five minutes took place. For the blocking step, a solution of 0,1% BSA (SERVA Elektrophoresis GmbH) diluted in PBS and 20% of goat serum (Sigma-Aldrich Chemie, GmbH) was prepared. 200 µL of the blocking solution was then applied to each spleen section and incubated for 30 minutes at room temperature. A washing step with PBS of five minutes was then performed.

The following reagents were obtained through the NIH Tetramer Core Facility (Emory University, Atlanta, GA): PE-labelled mouse mCD1d PBS-57 tetramer reagent and mouse CD1d unloaded. These last-mentioned were diluted in 0.1% BSA and 20% of goat serum with a dilution factor of 1:50 (see above). 200 µL of the solution was applied onto each sample and incubated for 60 minutes at room temperature in the dark. After three washing steps of five minutes three times in the dark, the tissue sections were dipped into distilled water. To protect fluorescent dyes and achieve a brighter signal, a drop of Prolong™ Diamond Antifade Mountant with DAPI (Thermo Fisher Scientific Inc., Carlsbad, CA, USA) was applied to the samples, which in turn were covered by a coverslip and sealed with nail polish. The tissue sections were incubated overnight at four degrees Celsius.

The quantitative evaluation was made by the use of CLSM by counting stained NKT cells in six HPF (400x magnification) followed by the calculation of a mean value of the six HPF for each sample.

2.9 Statistical Analysis

All results are presented as means ± standard error of the mean (SEM). Testing for normality was evaluated by the Kolmogorov-Smirnov test with Dallal-Wilkinson-Lillifors correction and the Shapiro-Wilk normality test. When comparing more than three groups with normal

distribution and homogeneity of variance, an analysis of variance (ANOVA) was used. In the case of significance, the Bonferroni post-hoc test to adjust for multiple testing is performed. When the homogeneity of variances assumption is not met, Welch's ANOVA test is used. If the distribution of the measured values is not normal, a non-parametrical technique such as the Kruskal-Wallis test is performed. P-value < 0.05 was considered statistically significant. All statistical analysis were performed using IBM SPSS-Statistics 26.0 (SPSS Inc., Chicago, IL, USA). The creation of the graphics was done with Prism 9 for macOS (GraphPad Software, LLC, La Jolla, CA, USA).

3 Results

3.1 Disease severity of vehicle, BAF-312 and A-971437 in NTS

NTS was induced in vehicle treated mice, BAF-312 treated mice and mice treated with A-971432 and disease activity was evaluated after 9 days. On day 0 as well as on day 9 after NTS induction, albuminuria in the three groups has been evaluated by the measurement of the albumin-to-creatinine ratio (Chapter 2.4). Very low and not significantly different albuminuria levels were detected in the three comparing groups at day 0 (Figure 8). After the NTS-induction and the once-daily therapy up until day 9, mice treated with A-971432 had similar and not statistically different albuminuria levels as compared to vehicle-treated and BAF-312-treated mice (Figure 8). This trend towards higher albuminuria in mice treated with BAF-312 is probably driven due to an outliner.

We further evaluated histopathology by evaluation of PAS-stained kidney sections. When PAS-score of all three groups were evaluated (Chapter 2.6), no statistically significant differences between the vehicle group, the BAF-312 group and the A-974132 group were detected. Furthermore, tubular casts as representatives of tubular injury were quantified. Interestingly, A-971432-treated mice had lower numbers of tubular casts as compared to

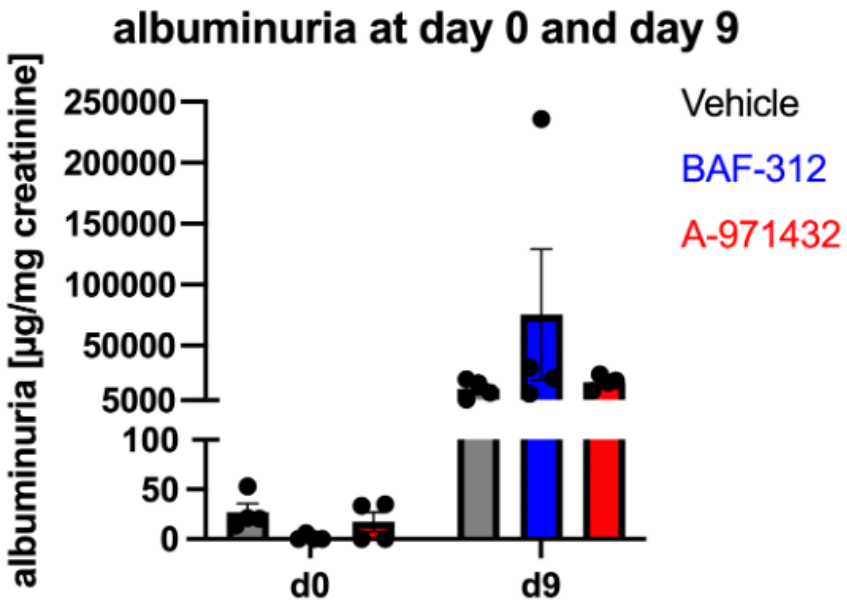

Figure 8: Albuminuria a day 0 (before NTS induction and treatment) and day 9 (after NTS induction)

Urine albumin excretion is indicated in µg per mg of urinary creatinine. ***(a)*** *Mice before NTS induction and treatment with vehicle (n=4), BAF-312 (n=4) or A-971432 (n=4). Data (mean ± SEM) for urinary albumin-to-creatinine ratio on day 0: vehicle = 27,06 ± 8,86 µg/mg, BAF-312 = 1,47 ± 1,45 µg/mg, A-971432 = 17,25 ± 9,95 µg/mg.* ***(b)*** *Mice received an once-daily treatment with either vehicle (n=4), BAF-312 (n=4) or A-971432 (n=4) until day 9. Data (mean ± SEM) for urinary albumin-to-creatinine ratio on day 9: Vehicle = 14334 ± 3777 µg/mg, BAF-312 = 75180 ± 53735 µg/mg, A-971432 = 19799 ± 2775 µg/mg.*

vehicle treated mice and mice treated with BAF-312 although no significance was detected (Figure 9).

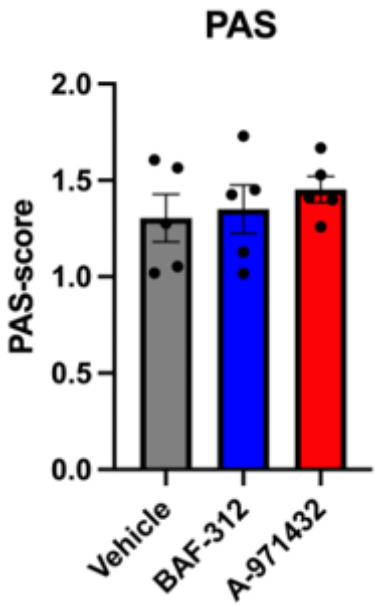

a PAS-Score

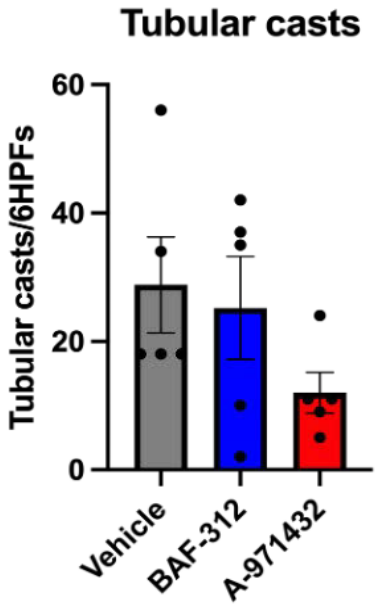

b Tubular casts

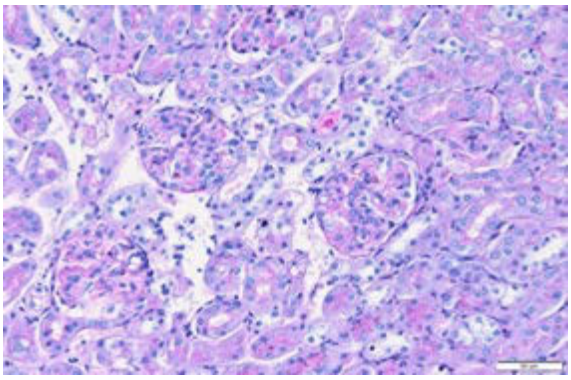

c Vehicle

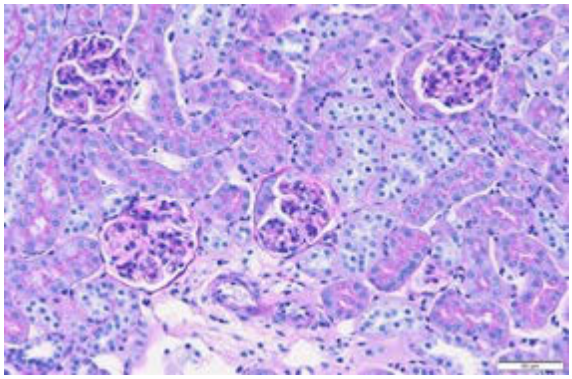

d BAF-312

Figure 9: Histopathologic changes in nephritic mice treated with vehicle, BAF-312 and A-971432

(a) PAS Score. *Raw data (mean ± SEM) of evaluated PAS-Score: vehicle (n=5) = 1,30 ± 0,12, BAF-312 (n=5) = 1,35 ± 0,13, A-971432 (n=5) = 1,45 ± 0.07.* ***(b) Tubular casts****. Tubular injury evaluated in 6 HPFs per kidney section. (mean ± SEM) of tubule casts: vehicle (n=5) = 28,80 ± 7,47, BAF-312 (n=5) = 25,20 ± 8,02, A-971432 (n=5) = 12,00 ± 3,19 PAS-stained kidney sections of vehicle* ***(c)****, BAF-312* ***(d)****, and A-971432 mice* ***(e)****.*

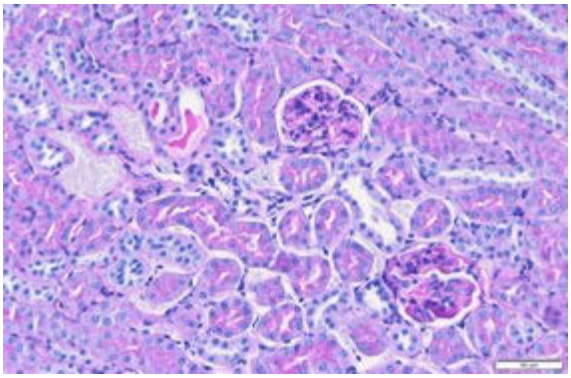

e A-971432

3.2 B cell immune response in vehicle, BAF-312 and A-971432

For the relative evaluation of the B-cell immune response after NTS-induction, the circulating autologous antibodies against induced heterologous rabbit antibodies have been measured photometrically (Chapter 2.5). Interestingly, the anti-rabbit-IgG serum titre didn't show statistically significant differences between the negative control group receiving vehicle, the positive control group treated with the non-selective S1P modulator BAF-312 and the mice injected with A-971432 9 days after NTS-induction (Figure 10). It can therefore be assumed, that the injection with S1P modulators, including BAF-312 and A-971432, did not influence the antibody production in the model of NTS.

Figure 10: Titre determination of anti-rabbit-IgG in mouse serum at day 9

Anti-rabbi-IgG serum titre was determined by the photometrical measurement of OD at a wavelength of 450 nm (dilution 1:3200). The means of OD of vehicle mice (n=4), BAF-312 mice (n=4) and A-971432 mice (n=4) didn't differ statistically. Blank corrected average (mean ± SEM) of OD): vehicle= 1,11 ± 0.35, BAF-312 = 0,81 ± 0.34, A-971432 = 1,02 ± 0.25.

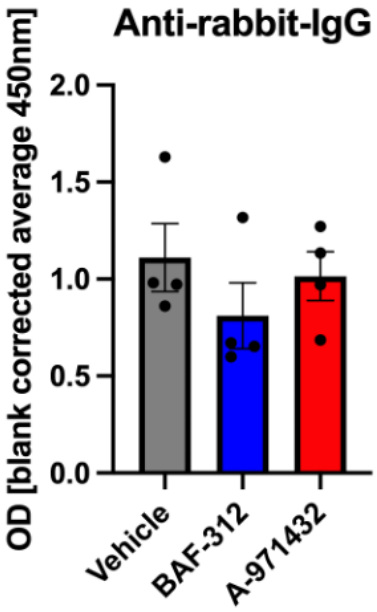

3.3 Immunohistochemical stainings showed different numbers of kidney infiltrating immune cells

NTS is critically mediated by $CD4^+$ T cells, as well as kidney infiltrating macrophages and neutrophils. For the evaluation of immune cell infiltration in the kidney, immunohistochemical staining of tissue sections were performed to quantify $CD4^+$ and $CD8^+$ T cells as well as infiltrating macrophages and neutrophils expressing CD68 and Ly6G respectively (Chapter 2.7). Comparing the three groups treated either with vehicle, with BAF-312 or with A971432, BAF-312 treated mice showed a statistically significant decreased number of $CD4^+$ T cells compared to the negative control (vehicle) group ($p = 0.014$) and to the A-971432 group ($p = 0.014$). $CD8^+$ T cells were also significantly decreased in BAF-312 mice compared to A-971432 mice ($p = 0.004$). A statically significant difference between BAF-312 and the vehicle group was not detected (Figure 11, Figure 12).

Four LPFs of $CD68^+$ stained kidney sections were evaluated for each sample. When comparing the mean scores of $CD68^+$ cells in each group, no statistically differences between the vehicle, BAF-312 and the A-971432 mice were evaluated. The means of counted Ly6G stained cells in six HPFs in kidney sections of the three groups didn't show any statistically significant differences either (Figure 13, Figure 14).

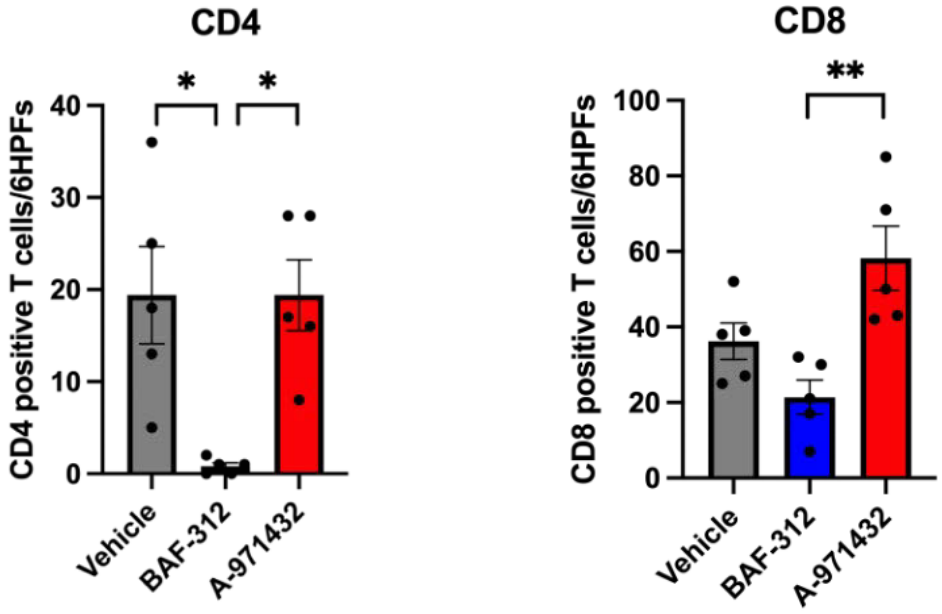

a *$CD4^+$ T cells* ***b*** *$CD8^+$ T cells*

Figure 11: Kidney infiltrating $CD4^+$ and $CD8^+$ T cells

$CD4^+$ T cells and $CD8^+$ T cells were evaluated by immunohistochemical staining from kidneys of vehicle, BAF-312 and A-971432 mice. ***(a)*** *Raw data (mean ± SEM) of counted $CD4^+$ T cells per 6 HPFs: vehicle (n=5) = 19,40 ± 5,28, BAF-312 (n=5) = 0,80 ± 0.37, A-971432 (n=5) = 19,40 ± 3.84.* ***(b)*** *Raw data (mean ± SEM) of counted $CD8^+$ T cells per 6 HPFs: vehicle (n=5) = 36,20 ± 4,85, BAF-312 (n=5) = 21,40 ± 4,55, A-971432 (n=5) = 58,20 ± 8,49. * $p < 0.05$, ** $p < 0.005$.*

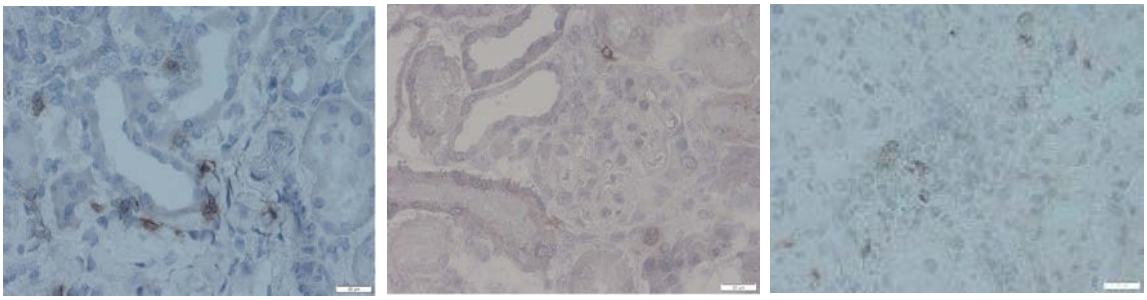

a *$CD8^+$ in vehicle* ***b*** *$CD8^+$ in BAF-312* ***c*** *$CD8^+$ in A-971432*

Figure 12: Representative micrographs of immunohistochemical stainings

$CD8^+$ T cells in ***(a)*** *vehicle* ***(b)*** *BAF-312 and* ***(c)*** *A-971432 mice (x400).*

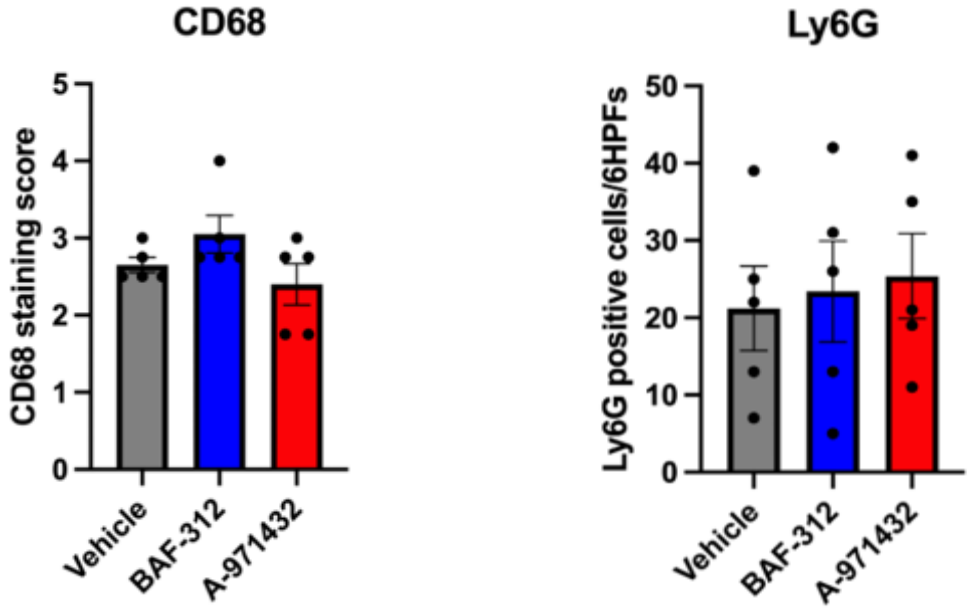

a *CD68⁺ cells* ***b*** *Ly6G cells*

Figure 13: Immunohistochemical staining of CD68 and Ly6G in kidney

(a*)* *Semiquantitative staining score for CD68⁺cell. Data given as mean ± SEM of counted CD68⁺ cells per 4 LPFs (x200): vehicle (n=5) = 2,68 ± 0,12, BAF-312 (n=5) = 3,05 ± 0,24, A-971432 (n=5) = 2,40 ± 0,27.* ***(b)*** *Mean ± SEM of Ly6G positive cells in 6 HPFs (x400): vehicle (n=5) = 21,20 ± 5,48, BAF-312 (n=5) = 23,40 ± 6,55, A-971432 (n=5) = 25,40 ± 5,49.*

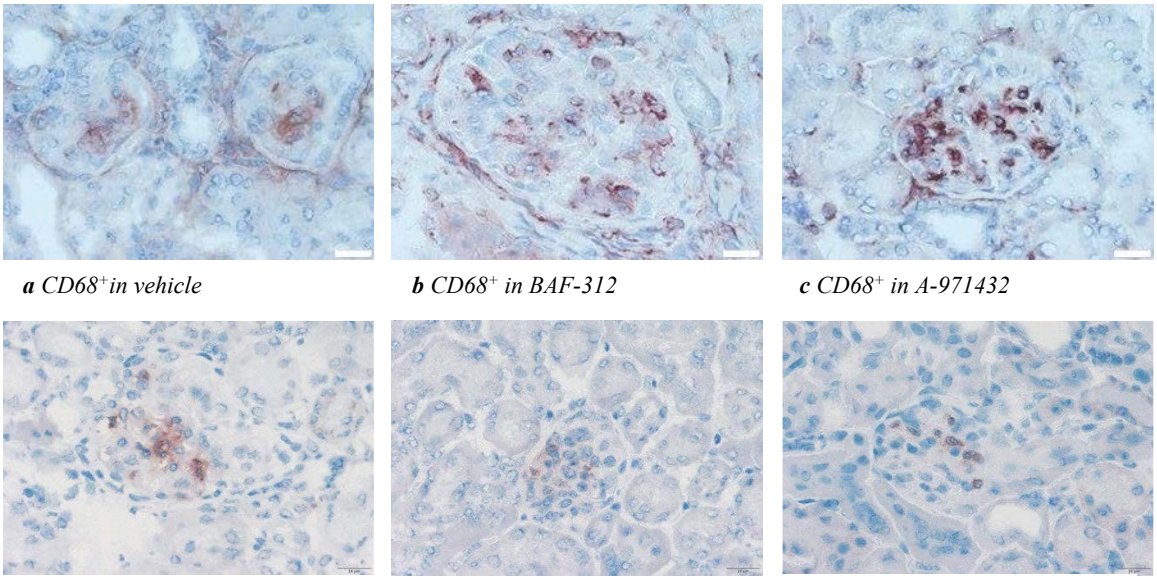

a *CD68⁺in vehicle* ***b*** *CD68⁺ in BAF-312* ***c*** *CD68⁺ in A-971432*

d *Ly6G in vehicle* ***e*** *Ly6G in BAF-312* ***f*** *Ly6G in A-971432*

Figure 14: Representative micrographs of immunohistochemical stainings of CD68+ and Ly6G cells

CD68⁺ stained cells in vehicle ***(a)****, BAF-312* ***(b)*** *and A-971432 mice* ***(c)*** *(x200) and Ly6G stained cells in vehicle* ***(d)****, BAF-312* ***(e)*** *and A-971432 mice* ***(f)*** *(x400).*

3.4 Evaluation of NKT cells in NTS

Our preliminary results from flow cytometry (data not shown) suggested that treatment with BAF-312 and A-971432 might influence numbers of NK and NKT cells in NTS. Therefore, evaluation of NKT cells in spleen sections, using a CD1d PBS-57 tetramer staining was performed. Under CLSM the stained cells were counted in six HPFs per tissue section and a

Figure 16: CD1d PBS-57 tetramer staining of NKT cells in spleen

*Data are given as mean ± SEM of counted CD1d PBS-57 positive cells in 6 HPFs for each evaluated group: vehicle (n=5) = 15,20 ± 2,78, BAF-312 (n=5) = 29,00 ± 3,78, A-971432 (n=5) = 14,80 ± 1,77. * p < 0.05.*

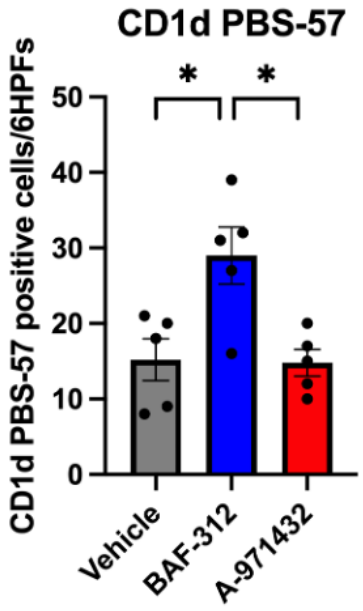

Figure 15: Exemplary illustration of CD1d PBS-57 tetramer stained NKT cells evaluated under confocal laser scanning microscopy

*CD1d PBS-57 tetramer NKT cells in vehicle **(a)**, BAF-312 **(b)**, A-971432 **(c)** and unloaded tetramer control tissue section **(d)** (x400).Blue: DAPI; Red: CD1d PBS-57.*

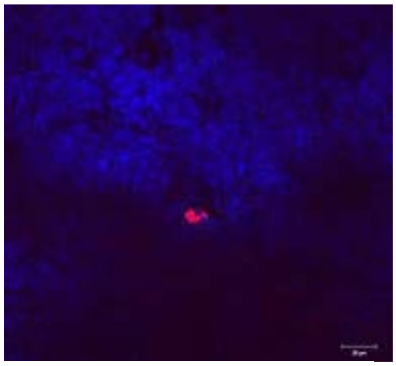

***a** Vehicle*

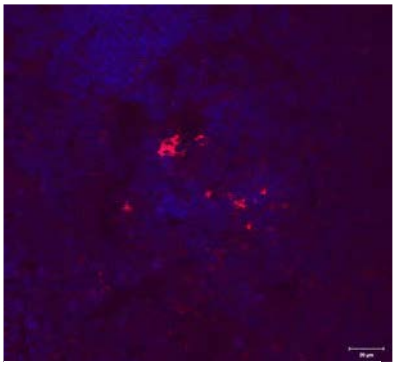

***b** BAF-312*

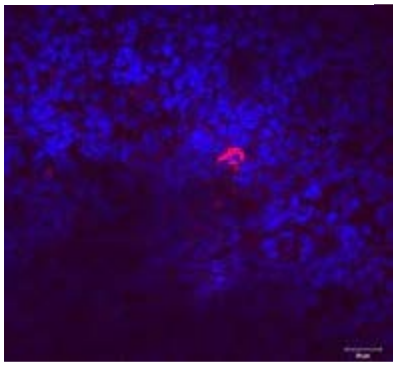

***c** A-971432*

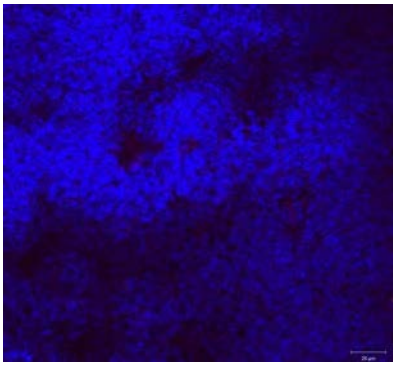

***d** Unloaded tetramer control*

mean for the vehicle, BAF-312 and A-971432 group was calculated. Mice treated with BAF-312 presented a statistically significant increased number of CD1d PBS-57 stained cells compared to the vehicle group ($p = 0.017$) as well as to the A-971432 group ($p = 0.014$) (Figure 15, Figure 16).

4 Discussion

NTS is a well-described murine model of immune complex RPGN. In the pathogenesis of NTS, lymphocytes are of particularly importance. Th cells, including Th1 and Th17 as well as neutrophils and macrophages infiltrate the kidney and contribute to local tissue damage and crescents formations within the glomeruli (134,138).

The receptor S1P1, one of the five known S1PRs which is mainly expressed on the surface of T and B cells, seems to be important for the emigration of activated lymphocytes from the secondary lymph organs to the site of injury (170).

Fingolimod (FTY720) was detected as a functional antagonist of S1P1 as well as of S1P2 and S1P5. By activating S1P1, fingolimod leads to internalization and degradation of this receptor and consequently to a decrease of lymphocytes in the periphery (171). Nowadays, fingolimod and the next generation S1P modulator siponimod (BAF-312), which is selective for S1P1 and S1P5, are potent drugs for the treatment of MS (172,174).

Interestingly, in various mice model of GN, fingolimod also showed an inhibitory effect on the progression of GN (175–177). Wolf et al. showed that fingolimod potentially inhibits Treg proliferation and thus their immunosuppressive activity in the NTS model (178). Importantly, Tregs were isolated and treated *in vitro* with fingolimod. After fingolimod pretreatment, Tregs lost their suppressive capacity when transferred into mice subjected to NTS. Still, the systemic effect of fingolimod with a focus on its action on S1P5 in the development of NTS has not been elucidated so far.

For this reason, rather than evaluating unselective S1P functional antagonists such as fingolimod or Siponimod, we aimed to investigate the influence of a selective S1P5 agonist on the pathogenesis of NTS in this study.

S1P5 is mainly expressed on oligodendrocytes and brain endothelial cells (179,180). At the present time, there is still a lack of specific and sensitive antibodies targeting S1P5, which prevented us to conduct direct immunohistochemical stainings of S1P5. Thus, we currently lack exact receptor locations in tissues involved in the pathogenesis of NTS such as kidney, spleen and draining lymph nodes. Van Doorn et al. showed that the activation of S1P5 leads to an improved integrity of the blood-brain barrier and a decreased transendothelial passing of monocytes in vitro thereby resulting in less overt inflammation (179). Abbvie developed a highly selective agonist for S1P5 named A-971432, which accumulates in plasma and the CNS after oral dosing in various species used in preclinical studies. Furthermore, they found that A-971432 improved blood-brain barrier integrity *in vitro* and had a protective effect of

age-related cognitive impairment in mice. Treatment with A-971432 is therefore handled as a possible new option in neurodegenerative disorders (206).

In preliminary experiments as described above (Chapter 1.4), mRNA expression levels of S1P5 were highly increased in mice in the NTS model compared to the healthy control group (data not shown). In initial NTS experiments in S1P5 deficient mice (data not shown), significant decreased albuminuria on day 7 in S1P5-deficient mice was detected compared to wild-type mice. These results compelled us to conduct a trial in the NTS model to compare mice treated with A-971432, a selective S1P5 agonist, with mice which received an unselective S1PR agonist (BAF-312). Our negative control group was treated with vehicle. Albuminuria levels were not significantly different in the three groups, although we detected higher values in BAF-312 treated mice as compared to vehicle treated mice and mice treated with A-971432. These higher albuminuria levels in mice treated with BAF-312 are probably due to an outliner. But there could also be another reason for this higher trend of albuminuria in BAF-312-treated mice. Interestingly, it has been shown that FTY720, the predecessor of BAF-312, does not act as a functional receptor antagonist at the onset of therapy but as an unselective S1P receptor agonist leading to an increased proinflammatory response. Only after a longer period of time, FTY720 starts performing the role as functional receptor antagonist by the degradation of S1P receptors (207). This was shown, among others, in a rat model of albumin overload-induced nephropathy where rats treated with FTY720 had decreased tubulointerstitial inflammation after nine weeks (208). These two modes of actions of FTY720 could probably also explain our increase of albuminuria in the BAF-312 group at day 9 of treatment. Consequently, it would be interesting to investigate whether albuminuria decreases in the BAF-312 group, if the duration of treatment in our experiments is prolonged.

Determination of anti-rabbit-IgG titre in the mouse serum was performed to evaluate the effect of the S1PR modulators on the B cell immune response. As the results did not show statistically significant differences between the three groups, it can be assumed that selective and unselective S1PR modulators do not influence the B cell activity in the NTS model.

As far as for PAS stainings, no statistically significant differences comparing PAS-score as well as the number of tubular casts in kidney tissue sections were detected. Nevertheless, mice treated with A-971432 tended to have less tubular injury compared to the negative and positive control group. This might indicate an effect of A-971432 on tubular cells and thus, tubular cell necrosis in the context of acute renal injury. Furthermore, Wünsche et al. detected that depletion of S1P5 resulted in an antifibrotic effect and inhibited the TGF-β2-

mediated expression of the connective tissue growth factor (CTGF) in vitro (182). Since treatment in our hands was too short to induce fibrosis in the NTS model, we need to evaluate a possible anti-fibrotic effect of A-971432 in the NTS model in the future. These experiments need to include sirius red staining or the detection of anti-smooth muscle antibodies (ASMA) by indirect immunofluorescence technique.

Our immunohistochemical stainings revealed significantly decreased $CD4^+$ T cells infiltrating kidneys of mice treated with BAF-312 as compared to the two other groups. Furthermore, mice treated with BAF-312 also showed a significant lower number of $CD8^+$ T cells in relation to the A-971432 group. Comparing BAF-312 to the vehicle group, no statistically significant differences were detected although BAF-312 treated mice again showed a considerable lower number of $CD8^+$ T cells. These findings reflect the fact that BAF-312 targets not only S1P5 but also S1P1 leading to a decreased migration of T cells to the inflamed tissue (170). In our trial, A-971432 seems not to a have a potent effect on T cells since the detected numbers of $CD4^+$ and $CD8^+$ T cells infiltrating the kidney are comparable to those in the vehicle group. Thus, the effect of BAF-312 on T cell migration in our model seems to be primarily orchestrated via S1P1. Evaluation of kidney infiltrating macrophages and neutrophils showed no statistical significant difference between treatment with the two S1PR modulators and vehicle.

Flow cytometry analysis of kidney and spleen (not further described in this diploma thesis) was performed by Katharina Artinger. A statistically significant increased number of NKT cells in the spleen of the A-971432 group as well as of the BAF-312 group was detected compared to the vehicle control group. In line, Wang et al. reported an increased proportion of iNKT cells in the spleen after a S1P treatment in a Coxsackie B3-induced myocarditis mouse model, which was associated with decreased myocardial inflammation. They assumed that S1P induces upregulation of S1P1 as well as an increase of iNKT cells in the spleen, which in turn exert an anti-inflammatory role in this animal model (209). Nevertheless, they only investigated the interaction between S1P and S1P1 whereas the other S1PRs 2-5 and their influences on NKT cells remain to be studied. A recently published study conducted by Ferror et al. revealed that MS patients treated with oral fingolimod for one year, showed an increased number of Tregs as well as regulatory subset of iNKT cells in peripheral blood (210). As a next step, it would be interesting to evaluate the effect of oral fingolimod on Tregs in the NTS model. Furthermore, the mechanisms of how S1P modulators affect iNKT cells in the NTS model remains unclear und needs to be further investigated.

With the aim to replicate these results detected in flow cytometry analysis, one aim of this study was to established a fluorescent CD1d-tetramer staining to further evaluate NKT cells in their spatial environment. We successfully identified fluorescently labelled iNKT cells in spleens of mice treated with vehicle, BAF-312 and A-971432. The evaluation using CSLM showed a statistically increased number of NKT cells in BAF-312 mice but not in mice treated with A-971432. However, these results should be considered with caution, since it has proved difficult to quantity the "real" NKT cells and not to confuse them with autofluorescent macrophages (211). Still, no positive signal was detected in isotype control staining.

Although the treatment with A-971432 did not result in a significant altered development of NTS compared to the vehicle group in our experiments, the possible antifibrotic effect of A-971432 should be further investigated as described above. Furthermore, considerable differences compared to the BAF-312 group have especially been detected with regard to the infiltrating immune cells into the kidney.

Further experiments in the NTS model should be performed by using S1P5-deficient (knock-out) mice and mice treated with the selective S1P5 agonist A-971432. Importantly, treatment needs to be prolonged to evaluate potential anti-fibrotic effects and to gain more information on their effects on pan-lymphocytes as well as NKT cells.

Taken together, A-971432 did not show significant differences in terms of albuminuria and infiltrating immune cells into the kidney compared to the vehicle group after 7 days of treatment. Nevertheless, BAF-312 and A-971432 seem to increase NKT cells in spleen, but their impact on the NTS model remains to be further investigated.

5 References

1. Lote CJ. Principles of Renal Physiology. 5th ed. New York: Springer Science & Business Media; 2012.

2. Mescher AL. Junqueira's Basic Histology: Text and Atlas. 14th ed. McGraw-Hill Education; 2015.

3. Bulger RE. Kidney Morphology: Update 1985. Toxicol Pathol. 1986;14(1):13–25.

4. Kurtz A, Pape HC, Silbernagl S. Physiologie. 8th ed. Stuttgart: Georg Thieme Verlag; 2018.

5. Falkson S. Anatomy, Abdomen and Pelvis, Bowman Capsule [Internet]. 2021 [cited 2022 Feb 16]. Available from: https://www.statpearls.com/articlelibrary/viewarticle/18488/

6. Kaufman DP, Basit H, Knohl SJ. Physiology, Glomerular Filtration Rate [Internet]. 2021 [cited 2022 Feb 16]. Available from: https://www.statpearls.com/ArticleLibrary/viewarticle/22278

7. Kidney Disease: Improving Global Outcomes (KDIGO) CKD Work Group. KDIGO 2012 Clinical Practice Guideline for the Evaluation and Management of Chronic Kidney Disease. Kidney inter, Suppl. 2013;3(1):1–150.

8. Shannon JA, Smith HW. The Excretion Of Inulin, Xylose And Urea By Normal And Phlorizinized Man. J Clin Invest. 1935;14(4):393–401.

9. Schwartz GJ, Furth SL. Glomerular filtration rate measurement and estimation in chronic kidney disease. Pediatr Nephrol. 2007;22(11):1839–48.

10. Couser WG. Glomerulonephritis. Lancet. 1999;353(9163):1509–15.

11. Chadban S, Atkins R. Glomerulonephritis. Lancet. 2005;365(9473):1797–806.

12. Sarnak MJ, Levey AS, Schoolwerth AC, Coresh J, Culleton B, Hamm LL, et al. Kidney Disease as a Risk Factor for Development of Cardiovascular Disease. Hypertens J Am Hear Assoc. 2003;42(5):1050–65.

13. Khanna R. Clinical presentation & management of glomerular diseases: hematuria, nephritic & nephrotic syndrome. Mo Med. 2011;108(1):33–6.

14. Hricik DE, Chung-Park M, Sedor JR. Glomerulonephritis. N Engl J Med. 1998;339(13):888–99.

15. Politano SA, Colbert GB, Hamiduzzaman N. Nephrotic Syndrome. Prim Care Clin Office Pract. 2020;47(4):597–613.

16. Lamba P, Nam KH, Contractor J, Kim A. Nephritic Syndrome. Prim Care Clin Office Pract. 2020;47(4):615–29.

17. Jennette JC, Thomas DB. Crescentic glomerulonephritis. Nephrol Dial Transpl. 2001;16(suppl_6):80–2.

18. Couser WG. Rapidly Progressive Glomerulonephritis: Classification, Pathogenetic Mechanisms, and Therapy. Am J Kidney Dis. 1988;11(6):449–64.

19. Andrassy K, Küster S, Waldherr R, Ritz E. Rapidly Progressive Glomerulonephritis: Analysis of Prevalence and Clinical Course. Nephron. 1991;59:206–12.

20. Jennette JC, Falk RJ, Bacon PA, Basu N, Cid MC, Ferrario F, et al. 2012 Revised International Chapel Hill Consensus Conference Nomenclature of Vasculitides. Arthritis Rheumatism. 2013;65(1):1–11.

21. Hudson BG, Tryggvason K, Sundaramoorthy M, Neilson EG. Alport's Syndrome, Goodpasture's Syndrome, and Type IV Collagen. New Engl J Med. 2003;348(25):2543–56.

22. Sanders JS, Rutgers A, Stegeman C, Kallenberg C. Pulmonary-Renal Syndrome with a Focus on Anti-GBM Disease. Semin Resp Crit Care. 2011;32(03):328–34.

23. Goodpasture EW. The Significance Of Certain Pulmonary Lesion In Relation To The Etiology Of Influenza. Am J Medical Sci. 1919;158(6):863–70.

24. Wilson CB, Dixon FJ. Anti-glomerular basement membrane antibody-induced glomerulonephritis. Kidney Int. 1973;3(2):74–89.

25. McAdoo SP, Pusey CD. Anti-Glomerular Basement Membrane Disease. Clin J Am Soc Nephro. 2017;12(7):1162–72.

26. Savage CO, Pusey CD, Bowman C, Rees AJ, Lockwood CM. Antiglomerular basement membrane antibody mediated disease in the British Isles 1980-4. Br Med J (Clin Res Ed). 1986;292(6516):301–4.

27. CB W. Goodpasture's Syndrome Associated with Influenza A2 Virus Infection. Ann Intern Med. 1972;76(1):91.

28. Donaghy M, Rees AJ. Cigarette Smoking And Lung Haemorraghe In Glomerulonephritis Caused By Autoantibodies To Glomerular Basement Membrane. Lancet. 1983;322(8364):1390–3.

29. GJ B, AA K. The association between hydrocarbon exposure and anti-glomerular basement membrane antibody-mediated disease (Goodpasture's syndrome). Am J Ind Med. 1992;21(2):141–53.

30. Fisher M, Pusey CD, Vaughan RW, Rees AJ. Susceptibility to anti-glomerular basement membrane disease is strongly associated with HLA-DRB1 genes. Kidney Int. 1997;51(1):222–9.

31. Lerner RA, Glassock RJ, Dixon FJ. The role of anti-glomerular basement membrane antibody in the pathogenesis of human glomerulonephritis. J Exp Medicine. 1967;126(6):989–1004.

32. Rutgers A, Meyers KEC, Canziani G, Kalluri R, Lin J, Madaio MP. High affinity of anti-GBM antibodies from Goodpasture and transplanted Alport patients to α3(IV)NC1 collagen. Kidney Int. 2000;58(1):115–22.

33. Turner N, Mason PJ, Brown R, Fox M, Povey S, Rees A, et al. Molecular cloning of the human Goodpasture antigen demonstrates it to be the alpha 3 chain of type IV collagen. J Clin Invest. 1992;89(2):592–601.

34. Saus J, Wieslander J, Langeveld JPM, Quinones S, Hudson BG. Identification of the Goodpasture Antigen as the a3(IV) Chain of Collagen IV. J Biol Chem. 1988;263:13374–80.

35. Hudson BG, Tryggvason K, Sundaramoorthy M, Neilson EG. Alport's Syndrome, Goodpasture's Syndrome, and Type IV Collagen. New Engl J Med. 2003;348(25):2543–56.

36. Netzer KO, Leinonen A, Boutaud A, Borza DB, Todd P, Gunwar S, et al. The Goodpasture Autoantigen. J Biol Chem. 1999;274(16):11267–74.

37. Pedchenko V, Bondar O, Fogo AB, Vanacore R, Voziyan P, Kitching AR, et al. Molecular Architecture of the Goodpasture Autoantigen in Anti-GBM Nephritis. New Engl J Med. 2010;363(4):343–54.

38. Chan AL, Louie S, Leslie KO, Juarez MM, Albertson TE. Cutting Edge Issues in Goodpasture's Disease. Clin Rev Allerg Immu. 2011;41(2):151–62.

39. Salant DJ. Goodpasture's Disease — New Secrets Revealed. New Engl J Medicine. 2010;363(4):388–91.

40. Wu J, Hicks J, Borillo J, Glass WF, Lou YH. CD4(+) T cells specific to a glomerular basement membrane antigen mediate glomerulonephritis. J Clin Investigation. 2002;109(4):517–24.

41. Dean EG, Wilson GRA, Li M, Edgtton KL, O'Sullivan KIMM, Hudson BG, et al. Experimental autoimmune Goodpasture's disease: A pathogenetic role for both effector cells and antibody in injury. Kidney Int. 2005;67(2):566–75.

42. Bolton WK, Innes DJ, Sturgill BC, Kaiser DL. T-cells and macrophages in rapidly progressive glomerulonephritis: Clinicopathologic correlations. Kidney Int. 1987;32(6):869–76.

43. Cui Z, Zhao M hui, Segelmark M, Hellmark T. Natural autoantibodies to myeloperoxidase, proteinase 3, and the glomerular basement membrane are present in normal individuals. Kidney Int. 2010;78(6):590–7.

44. Sheerin NS, Springall T, Carroll MC, Hartley B, Sacks SH. Protection against anti-glomerular basement membrane (GBM)-mediated nephritis in C3- and C4-deficient mice. Clin Exp Immunol. 1997;110(3):403–9.

45. Kitching AR, Tipping PG, Holdsworth SR. IL-12 directs severe renal injury, crescent formation and Th1 responses in murine glomerulonephritis. Eur J Immunol. 1999;29(1):1–10.

46. Timoshanko JR, Holdsworth SR, Kitching AR, Tipping PG. IFN-γ Production by Intrinsic Renal Cells and Bone Marrow-Derived Cells Is Required for Full Expression of Crescentic Glomerulonephritis in Mice. J Immunol. 2002;168(8):4135–41.

47. Kenneth M, Casey W. Janeway's Immunobiolody. 9th ed. New York, USA: Garland Science, Taylor & Francis Group, LLC; 2017. 762 p.

48. Kambham N. Postinfectious Glomerulonephritis. Adv Anat Pathol. 2012;19(5):338–47.

49. Yoshizawa N. Acute Glomerulonephritis. Internal Med. 2000;39(9):687–94.

50. Magistroni R, D'Agati VD, Appel GB, Kiryluk K. New developments in the genetics, pathogenesis, and therapy of IgA nephropathy. Kidney Int. 2015;88(5):974–89.

51. Rodrigues JC, Haas M, Reich HN. IgA Nephropathy. Clin J Am Soc Nephro. 2017;12(4):677–86.

52. Kiryluk K, Moldoveanu Z, Sanders JT, Eison TM, Suzuki H, Julian BA, et al. Aberrant glycosylation of IgA1 is inherited in both pediatric IgA nephropathy and Henoch–Schönlein purpura nephritis. Kidney Int. 2011;80(1):79–87.

53. Gharavi AG, Moldoveanu Z, Wyatt RJ, Barker CV, Woodford SY, Lifton RP, et al. Aberrant IgA1 Glycosylation Is Inherited in Familial and Sporadic IgA Nephropathy. J Am Soc Nephrol. 2008;19(5):1008–14.

54. McGrogan A, Franssen CFM, Vries CS de. The incidence of primary glomerulonephritis worldwide: a systematic review of the literature. Nephrol Dial Transpl. 2011;26(2):414–30.

55. Alchi B, Jayne D. Membranoproliferative glomerulonephritis. Pediatric Nephrol Berlin Ger. 2010;25(8):1409–18.

56. Sethi S, Fervenza FC. Membranoproliferative Glomerulonephritis — A New Look at an Old Entity. New Engl J Medicine. 2012;366(12):1119–31.

57. Weening JJ, D'Agati VD, Schwartz MM, Seshan SV, Alpers CE, Appel GB, et al. The Classification of Glomerulonephritis in Systemic Lupus Erythematosus Revisited. J Am Soc Nephrol. 2004;15(2):241–50.

58. Goules A, Masouridi S, Tzioufas AG, Ioannidis JPA, Skopouli FN, Moutsopoulos HM. Clinically Significant and Biopsy-Documented Renal Involvement in Primary Sjogren Syndrome. Medicine. 2000;79(4):241–9.

59. Sethi S, Zand L, Leung N, Smith RJH, Jevremonic D, Herrmann SS, et al. Membranoproliferative Glomerulonephritis Secondary to Monoclonal Gammopathy. Clin J Am Soc Nephro. 2010;5(5):770–82.

60. Stilmant MM, Bolton WK, Sturgill BC, Schmitt GW, Couser WG. Crescentic glomerulonephritis without immune deposits: Clinicopathologic features. Kidney Int. 1979;15(2):184–95.

61. Falk R, Jennette J. ANCA small-vessel vasculitis. JASN. 1997;2(8):314–22.

62. Jennette JC, Thomas DB. Crescentic glomerulonephritis. Nephrol Dial Transpl. 2001;16(suppl_6):80–2.

63. Jennette JC, Nachman PH. ANCA Glomerulonephritis and Vasculitis. Clin J Am Soc Nephro. 2017;12(10):1680–91.

64. Cornec D, Gall ECL, Fervenza FC, Specks U. ANCA-associated vasculitis — clinical utility of using ANCA specificity to classify patients. Nat Rev Rheumatol. 2016;12(10):570–9.

65. Witko-Sarsat V, Cramer E, Hieblot C, Guichard J, Nusbaum P, Lopez S, et al. Presence of proteinase 3 in secretory vesicles: evidence of a novel, highly mobilizable intracellular pool distinct from azurophil granules. Blood. 1999;94(7):2487–96.

66. Kallenberg CGM. Pathogenesis of ANCA-associated vasculitides. Ann Rheum Dis. 2011;70(Suppl 1):i59.

67. Unizony S, Villarreal M, Miloslavsky EM, Lu N, Merkel PA, Spiera R, et al. Clinical outcomes of treatment of anti-neutrophil cytoplasmic antibody (ANCA)-associated vasculitis based on ANCA type. Ann Rheum Dis. 2016;75(6):1166.

68. Lionaki S, Blyth ER, Hogan SL, Hu Y, Senior BA, Jennette CE, et al. Classification of antineutrophil cytoplasmic autoantibody vasculitides: The role of antineutrophil cytoplasmic autoantibody specificity for myeloperoxidase or proteinase 3 in disease recognition and prognosis. Arthritis Rheumatism. 2012;64(10):3452–62.

69. Jennette JC, Xiao H, Falk R, Gasim AMH. Experimental Models of Vasculitis and Glomerulonephritis Induced by Antineutrophil Cytoplasmic Autoantibodies. Contrib Nephrol. 2011;169:211–20.

70. Roth AJ, Ooi JD, Hess JJ, Timmeren MM van, Berg EA, Poulton CE, et al. Epitope specificity determines pathogenicity and detectability in ANCA-associated vasculitis. J Clin Invest. 2013;123(4):1773–83.

71. Brinkmann V, Reichard U, Goosmann C, Fauler B, Uhlemann Y, Weiss DS, et al. Neutrophil Extracellular Traps Kill Bacteria. Science. 2004;303(5663):1532–5.

72. Jones BE, Yang J, Muthigi A, Hogan SL, Hu Y, Starmer J, et al. Gene-Specific DNA Methylation Changes Predict Remission in Patients with ANCA-Associated Vasculitis. J Am Soc Nephrol. 2017;28(4):1175–87.

73. Söderberg D, Segelmark M. Neutrophil Extracellular Traps in ANCA-Associated Vasculitis. Front Immunol. 2016;7:256.

74. Moroni G, Ponticelli C. Rapidly progressive crescentic glomerulonephritis: Early treatment is a must. Autoimmun Rev. 2014;13(7):723–9.

75. Lockwood CM, Pearson TA, Rees AJ, Evans DJ, Peters DK, Wilson CB. Immunosuppression and plasma-exchange in the treatment of Goodpasture's syndrome. Lancet. 1976;307(7962):711–5.

76. Mukhtyar C, Flossmann O, Hellmich B, Bacon P, Cid M, Cohen-Tervaert JW, et al. Outcomes from studies of antineutrophil cytoplasm antibody associated vasculitis: a systematic review by the European League Against Rheumatism systemic vasculitis task force. Ann Rheum Dis. 2008;67(7):1004.

77. Westman KW, Bygren PG, Olsson H, Ranstam J, Wieslander J. Relapse rate, renal survival, and cancer morbidity in patients with Wegener's granulomatosis or microscopic polyangiitis with renal involvement. J Am Soc Nephrol. 1998;9(5):842–52.

78. Reinhold-Keller E, Beuge N, Latza U, Groot KD, Rudert H, Nölle B, et al. An interdisciplinary approach to the care of patients with Wegener's granulomatosis: Long-term outcome in 155 patients. Arthritis Rheumatism. 2000;43(5):1021–32.

79. Jayne D, Rasmussen N, Andrassy K, Bacon P, Tervaert JWC, Dadoniené J, et al. A Randomized Trial of Maintenance Therapy for Vasculitis Associated with Antineutrophil Cytoplasmic Autoantibodies. New Engl J Medicine. 2003;349(1):36–44.

80. Touzot M, Poisson J, Faguer S, Ribes D, Cohen P, Geffray L, et al. Rituximab in anti-GBM disease: A retrospective study of 8 patients. J Autoimmun. 2015;60:74–9.

81. Houssiau FA, Vasconcelos C, D'Cruz D, Sebastiani GD, Garrido E de R, Danieli MG, et al. Immunosuppressive therapy in lupus nephritis: The Euro-Lupus Nephritis Trial, a randomized trial of low-dose versus high-dose intravenous cyclophosphamide. Arthritis Rheumatism. 2002;46(8):2121–31.

82. Ginzler EM, Dooley MA, Aranow C, Kim MY, Buyon J, Merrill JT, et al. Mycophenolate Mofetil or Intravenous Cyclophosphamide for Lupus Nephritis. New Engl J Medicine. 2005;353(21):2219–28.

83. Houssiau FA, D'Cruz D, Sangle S, Remy P, Vasconcelos C, Petrovic R, et al. Azathioprine versus mycophenolate mofetil for long-term immunosuppression in lupus nephritis: results from the MAINTAIN Nephritis Trial. Ann Rheum Dis. 2010;69(12):2083.

84. Wofsy D, Diamond B, Houssiau FA. Commentary: Crossing the Atlantic: The Euro-Lupus Nephritis Regimen in North America. Arthritis Rheumatol. 2015;67(5):1144–6.

85. Montigny PM, Houssiau FA. New Treatment Options in Lupus Nephritis. Arch Immunol Ther Ex. 2022;70(1):11.

86. EMA. Benlysta [Internet]. 2021 [cited 2022 Apr 15]. Available from: https://www.ema.europa.eu/en/medicines/human/EPAR/benlysta

87. Furie R, Rovin BH, Houssiau F, Malvar A, Teng YKO, Contreras G, et al. Two-Year, Randomized, Controlled Trial of Belimumab in Lupus Nephritis. New Engl J Med. 2020;383(12):1117–28.

88. Mukhtyar C, Guillevin L, Cid MC, Dasgupta B, Groot K de, Gross W, et al. EULAR recommendations for the management of primary small and medium vessel vasculitis. Ann Rheum Dis. 2009;68(3):310.

89. Jones RB, Tervaert JWC, Hauser T, Luqmani R, Morgan MD, Peh CA, et al. Rituximab versus Cyclophosphamide in ANCA-Associated Renal Vasculitis. New Engl J Medicine. 2010;363(3):211–20.

90. Clain JM, Specks U. S1. Rituximab for ANCA-associated vasculitis: The experience in the United States. La Press Médicale. 2013;42(4):530–2.

91. Cartin-Ceba R, Golbin JM, Keogh KA, Peikert T, Sánchez-Menéndez M, Ytterberg SR, et al. Rituximab for remission induction and maintenance in refractory granulomatosis with polyangiitis (Wegener's): Ten-year experience at a single center. Arthritis Rheumatism. 2012;64(11):3770–8.

92. Guillevin L, Pagnoux C, Karras A, Khouatra C, Aumaître O, Cohen P, et al. Rituximab versus Azathioprine for Maintenance in ANCA-Associated Vasculitis. New Engl J Medicine. 2014;371(19):1771–80.

93. Smith RM, Jones RB, Specks U, Bond S, Nodale M, Aljayyousi R, et al. Rituximab as therapy to induce remission after relapse in ANCA-associated vasculitis. Ann Rheum Dis. 2020;79(9):1243–9.

94. Walsh M, Merkel PA, Peh CA, Szpirt WM, Puéchal X, Fujimoto S, et al. Plasma Exchange and Glucocorticoids in Severe ANCA-Associated Vasculitis. New Engl J Med. 2020;382(7):622–31.

95. Jayne DRW, Merkel PA, Schall TJ, Bekker P, Group AS. Avacopan for the Treatment of ANCA-Associated Vasculitis. New Engl J Med. 2021;384(7):599–609.

96. Chapter 2: General principles in the management of glomerular disease. Kidney Int Suppl. 2012;2(2):156–62.

97. Herold G. Innere Medizin. Köln: Gerd Herold; 2020.

98. Levy JB, Turner AN, Rees AJ, Pusey CD. Long-Term Outcome of Anti–Glomerular Basement Membrane Antibody Disease Treated with Plasma Exchange and Immunosuppression. Ann Intern Med. 2001;134(11):1033.

99. Heilman RL, Offord KP, Holley KE, Velosa JA. Analysis of risk factors for patient and renal survival in crescentic glomerulonephritis. American Journal of Kidney Diseases. 1987;9(2):98–207.

100. Hogan SL, Nachman PH, Wilkman AS, Jennette JC, Falk RJ. Prognostic markers in patients with antineutrophil cytoplasmic autoantibody-associated microscopic polyangiitis and glomerulonephritis. JASN. 1996;7(1):23–32.

101. Ponticelli C, Imbasciati E, Brancaccio D, Tarantino A, Rivolta E. Acute renal failure in systemic lupus erythematosus. Br Med J. 1974;3(5933):716–9.

102. Berden AE, Ferrario F, Hagen EC, Jayne DR, Jennette JC, Joh K, et al. Histopathologic Classification of ANCA-Associated Glomerulonephritis. J Am Soc Nephrol. 2010;21(10):1628–36.

103. Brubaker SW, Bonham KS, Zanoni I, Kagan JC. Innate Immune Pattern Recognition: A Cell Biological Perspective. Annu Rev Immunol. 2014;33(1):1–34.

104. Schatz DG, Ji Y. Recombination centres and the orchestration of V(D)J recombination. Nat Rev Immunol. 2011;11(4):251–63.

105. Witko-Sarsat V, Rieu P, Descamps-Latscha B, Lesavre P, Halbwachs-Mecarelli L. Neutrophils: Molecules, Functions and Pathophysiological Aspects. Lab Invest. 2000;80(5):617–53.

106. Furth R van, Cohn ZA, Hirsch JG, Humphrey JH, Spector WG, Langevoort HL. The mononuclear phagocyte system: a new classification of macrophages, monocytes, and their precursor cells. B World Health Organ. 1972;46(6):845–52.

107. Campbell KS, Hasegawa J. NK cell biology: An update and future directions. J Allergy Clin Immunol. 2013;132(3):536–544.

108. Parkin J, Cohen B. An overview of the immune system. Lancet. 2001;357(9270):1777–89.

109. Rudolph MG, Stanfield RL, Wilson IA. How TCRs Bind MHCs, Peptides, And Coreceptors. Annu Rev Immunol. 2006;24(1):419–66.

110. Neefjes J, Jongsma MLM, Paul P, Bakke O. Towards a systems understanding of MHC class I and MHC class II antigen presentation. Nat Rev Immunol. 2011;11(12):823–36.

111. Zhang N, Bevan MJ. CD8+ T Cells: Foot Soldiers of the Immune System. Immunity. 2011;35(2):161–8.

112. Caza T, Landas S. Functional and Phenotypic Plasticity of CD4+ T Cell Subsets. Biomed Res Int. 2015;2015:521957.

113. Raphael I, Nalawade S, Eagar TN, Forsthuber TG. T cell subsets and their signature cytokines in autoimmune and inflammatory diseases. Cytokine. 2015;74(1):5–17.

114. Stark JM, Tibbitt CA, Coquet JM. The Metabolic Requirements of Th2 Cell Differentiation. Front Immunol. 2019;10:2318.

115. Raphael I, Forsthuber TG. Stability of T-cell lineages in autoimmune diseases. Expert Rev Clin Immu. 2014;8(4):299–301.

116. Skurkovich S, Skurkovich B. Anticytokine Therapy, Especially Anti-Interferon-γ, as a Pathogenetic Treatment in TH-1 Autoimmune Diseases. Ann Ny Acad Sci. 2005;1051(1):684–700.

117. Jenkins MK, Moon JJ. The Role of Naive T Cell Precursor Frequency and Recruitment in Dictating Immune Response Magnitude. J Immunol. 2012;188(9):4135–40.

118. Godfrey DI, Uldrich AP, McCluskey J, Rossjohn J, Moody DB. The burgeoning family of unconventional T cells. Nat Immunol. 2015;16(11):1114–23.

119. Krovi SH, Gapin L. Invariant Natural Killer T Cell Subsets—More Than Just Developmental Intermediates. Front Immunol. 2018;9:1393.

120. O'Keeffe J, Podbielska M, Hogan EL. Invariant natural killer T cells and their ligands: focus on multiple sclerosis. Immunology. 2015;145(4):468–75.

121. Pietro C Di. The role of invariant NKT cells in organ-specific autoimmunity. Front Biosci. 2014;19(8):1240.

122. Lynch L, Michelet X, Zhang S, Brennan PJ, Moseman A, Lester C, et al. Regulatory iNKT cells lack expression of the transcription factor PLZF and control the homeostasis of Treg cells and macrophages in adipose tissue. Nat Immunol. 2015;16(1):85–95.

123. Rhost S, Sedimbi S, Kadri N, Cardell SL. Immunomodulatory Type II Natural Killer T Lymphocytes in Health and Disease. Scand J Immunol. 2012;76(3):246–55.

124. Melandri D, Zlatareva I, Chaleil RAG, Dart RJ, Chancellor A, Nussbaumer O, et al. The γδTCR combines innate immunity with adaptive immunity by utilizing spatially distinct regions for agonist selection and antigen responsiveness. Nat Immunol. 2018;19(12):1352–65.

125. Wu YL, Ding YP, Tanaka Y, Shen LW, Wei CH, Minato N, et al. γδ T Cells and Their Potential for Immunotherapy. Int J Biol Sci. 2014;10(2):119–35.

126. Schönefeldt S, Wais T, Herling M, Mustjoki S, Bekiaris V, Moriggl R, et al. The Diverse Roles of γδ T Cells in Cancer: From Rapid Immunity to Aggressive Lymphoma. Cancers. 2021;13(24):6212.

127. Hayday AC, Vantourout P. The Innate Biologies of Adaptive Antigen Receptors. Annu Rev Immunol. 2020;38(1):1–24.

128. Yazdanifar M, Barbarito G, Bertaina A, Airoldi I. γδ T Cells: The Ideal Tool for Cancer Immunotherapy. Cells. 2020;9(5):1305.

129. Nutt SL, Hodgkin PD, Tarlinton DM, Corcoran LM. The generation of antibody-secreting plasma cells. Nat Rev Immunol. 2015;15(3):160–71.

130. Keyt BA, Baliga R, Sinclair AM, Carroll SF, Peterson MS. Structure, Function, and Therapeutic Use of IgM Antibodies. Antibodies. 2020;9(4):53.

131. Sousa-Pereira P de, Woof JM. IgA: Structure, Function, and Developability. Antibodies. 2019;8(4):57.

132. Schroeder HW, Cavacini L. Structure and function of immunoglobulins. J Allergy Clin Immun. 2010;125(2):S41–52.

133. Thoenes GH. Glomerulonephritis. Curr Topics Pathol. 1976;61–106.

134. Artinger K, Kirsch AH, Aringer I, Moschovaki-Filippidou F, Eller P, Rosenkranz AR, et al. Innate and adaptive immunity in experimental glomerulonephritis: a pathfinder tale. Pediatric Nephrol Berlin Ger. 2016;32(6):943–7.

135. Odobasic D, Ghali JR, O'Sullivan KM, Holdsworth SR, Kitching AR. Glomerulonephritis Induced by Heterologous Anti-GBM Globulin as a Planted Foreign Antigen. Curr Protoc Immunol. 2014;106(1):15.26.1-15.26.20.

136. Du Y, Fu Y, Mohan C. Experimental anti-GBM nephritis as an analytical tool for studying spontaneous lupus nephritis. Arch Immunol Ther Ex. 2008;56(1):31–40.

137. Schrijver G, Bogman MJJT, Assmann KJM, Waal RMW de, Robben HCM, Gasteren H van, et al. Anti-GBM nephritis in the mouse: Role of granulocytes in the heterologous phase. Kidney Int. 1990;38(1):86–95.

138. Kurts C, Panzer U, Anders HJ, Rees AJ. The immune system and kidney disease: basic concepts and clinical implications. Nat Rev Immunol. 2013;13(10):738–53.

139. Turner JE, Krebs C, Tittel AP, Paust HJ, Meyer-Schwesinger C, Bennstein SB, et al. IL-17A Production by Renal γδ T Cells Promotes Kidney Injury in Crescentic GN. J Am Soc Nephrol. 2012;23(9):1486–95.

140. Krüger T, Benke D, Eitner F, Lang A, Wirtz M, Hamilton-Williams EE, et al. Identification and Functional Characterization of Dendritic Cells in the Healthy Murine Kidney and in Experimental Glomerulonephritis. J Am Soc Nephrol. 2004;15(3):613–21.

141. Korn T, Bettelli E, Oukka M, Kuchroo VK. IL-17 and Th17 Cells. Immunology. 2009;27(1):485–517.

142. Disteldorf EM, Krebs CF, Paust HJ, Turner JE, Nouailles G, Tittel A, et al. CXCL5 Drives Neutrophil Recruitment in TH17-Mediated GN. J Am Soc Nephrol. 2015;26(1):55–66.

143. Riedel JH, Paust HJ, Turner JE, Tittel AP, Krebs C, Disteldorf E, et al. Immature Renal Dendritic Cells Recruit Regulatory CXCR6+ Invariant Natural Killer T Cells to Attenuate Crescentic GN. J Am Soc Nephrol. 2012;23(12):1987–2000.

144. Tipping PG, Holdsworth SR. T Cells in Crescentic Glomerulonephritis. J Am Soc Nephrol. 2006;17(5):1253–63.

145. Niedermeier M, Reich B, Gomez MR, Denzel A, Schmidbauer K, Göbel N, et al. CD4+ T cells control the differentiation of Gr1+ monocytes into fibrocytes. Proc National Acad Sci. 2009;106(42):17892–7.

146. Miyara M, Sakaguchi S. Natural regulatory T cells: mechanisms of suppression. Trends Mol Med. 2007;13(3):108–16.

147. Sakaguchi S. Naturally arising Foxp3-expressing CD25+CD4+ regulatory T cells in immunological tolerance to self and non-self. Nat Immunol. 2005;6(4):345–52.

148. Kluger MA, Luig M, Wegscheid C, Goerke B, Paust HJ, Brix SR, et al. Stat3 Programs Th17-Specific Regulatory T Cells to Control GN. J Am Soc Nephrol. 2014;25(6):1291–302.

149. Ostmann A, Paust HJ, Panzer U, Wegscheid C, Kapffer S, Huber S, et al. Regulatory T Cell–Derived IL-10 Ameliorates Crescentic GN. J Am Soc Nephrol. 2013;24(6):930–42.

150. Wolf D, Hochegger K, Wolf AM, Rumpold HF, Gastl G, Tilg H, et al. CD4+CD25+ Regulatory T Cells Inhibit Experimental Anti-Glomerular Basement Membrane Glomerulonephritis in Mice. J Am Soc Nephrol. 2005;16(5):1360–70.

151. Eller K, Weber T, Pruenster M, Wolf AM, Mayer G, Rosenkranz AR, et al. CCR7 Deficiency Exacerbates Injury in Acute Nephritis Due to Aberrant Localization of Regulatory T Cells. J Am Soc Nephrol. 2010;21(1):42–52.

152. Förster R, Davalos-Misslitz AC, Rot A. CCR7 and its ligands: balancing immunity and tolerance. Nat Rev Immunol. 2008;8(5):362–71.

153. Tipping PG, Huang XR, Qi M, Van GY, Tang WW. Crescentic glomerulonephritis in CD4- and CD8-deficient mice. Requirement for CD4 but not CD8 cells. Am J Pathology. 1998;152(6):1541–8.

154. Couzi L, Merville P, Deminière C, Moreau J, Combe C, Pellegrin J, et al. Predominance of CD8+ T lymphocytes among periglomerular infiltrating cells and link to the prognosis of class III and class IV lupus nephritis. Arthritis Rheumatism. 2007;56(7):2362–70.

155. Heymann F, Meyer-Schwesinger C, Hamilton-Williams EE, Hammerich L, Panzer U, Kaden S, et al. Kidney dendritic cell activation is required for progression of renal disease in a mouse model of glomerular injury. J Clin Invest. 2009;119(5):1286–97.

156. Walport M. Complement. First of two parts. N Eng J Med. 2001;344(14):1058–66.

157. Thurman JM, Tchepeleva SN, Haas M, Panzer S, Boackle SA, Glogowska MJ, et al. Complement alternative pathway activation in the autologous phase of nephrotoxic serum nephritis. Am J Physiol-renal. 2012;302(12):F1529–36.

158. Quigg RJ, He C, Lim A, Berthiaume D, Alexander JJ, Kraus D, et al. Transgenic Mice Overexpressing the Complement Inhibitor Crry as a Soluble Protein Are Protected from Antibody-induced Glomerular Injury. J Exp Medicine. 1998;188(7):1321–31.

159. Turnberg D, Botto M, Warren J, Morgan BP, Walport MJ, Cook HT. CD59a Deficiency Exacerbates Accelerated Nephrotoxic Nephritis in Mice. J Am Soc Nephrol. 2003;14(9):2271–9.

160. Robson MG, Cook HT, Botto M, Taylor PR, Busso N, Salvi R, et al. Accelerated Nephrotoxic Nephritis Is Exacerbated in C1q-Deficient Mice. J Immunol. 2001;166(11):6820–8.

161. Ghosh T, Bian J, Gill D. Intracellular calcium release mediated by sphingosine derivatives generated in cells. Science. 1990;248(4963):1653–6.

162. Koch A, Pfeilschifter J, Huwiler A. Sphingosine 1-Phosphate in Renal Diseases. Cell Physiol Biochem. 2013;31(6):745–60.

163. Alemany R, Koppen CJ van, Danneberg K, Braak M ter, Heringdorf DM zu. Regulation and functional roles of sphingosine kinases. Naunyn-schmiedeberg's Archives Pharmacol. 2007;374(5–6):413–28.

164. Gennero I, Fauvel J, Niéto M, Cariven C, Gaits F, Briand-Mésange F, et al. Apoptotic Effect of Sphingosine 1-Phosphate and Increased Sphingosine 1-Phosphate Hydrolysis on Mesangial Cells Cultured at Low Cell Density∗. J Biol Chem. 2002;277(15):12724–34.

165. Hofmann LP, Ren S, Schwalm S, Pfeilschifter J, Huwiler A. Sphingosine kinase 1 and 2 regulate the capacity of mesangial cells to resist apoptotic stimuli in an opposing manner. Biol Chem. 2008;389(11):1399–407.

166. Klawitter S, Hofmann LP, Pfeilschifter J, Huwiler A. Extracellular nucleotides induce migration of renal mesangial cells by upregulating sphingosine kinase-1 expression and activity. Brit J Pharmacol. 2007;150(3):271–80.

167. Chiba K, Yanagawa Y, Masubuchi Y, Kataoka H, Kawaguchi T, Ohtsuki M, et al. FTY720, a novel immunosuppressant, induces sequestration of circulating mature lymphocytes by acceleration of lymphocyte homing in rats. I. FTY720 selectively decreases the number of circulating mature lymphocytes by acceleration of lymphocyte homing. J Immunol Baltim Md 1950. 1998;160(10):5037–44.

168. Yagi H, Kamba R, Chiba K, Soga H, Yaguchi K, Nakamura M, et al. Immunosuppressant FTY720 inhibits thymocyte emigration. Eur J Immunol. 2000;30(5):1435–44.

169. Brinkmann V, Davis MD, Heise CE, Albert R, Cottens S, Hof R, et al. The Immune Modulator FTY720 Targets Sphingosine 1-Phosphate Receptors. J Biol Chem. 2002;277(24):21453–7.

170. Matloubian M, Lo CG, Cinamon G, Lesneski MJ, Xu Y, Brinkmann V, et al. Lymphocyte egress from thymus and peripheral lymphoid organs is dependent on S1P receptor 1. Nature. 2004;427(6972):355–60.

171. Gräler MH, Goetzl EJ. The immunosuppressant FTY720 down-regulates sphingosine 1-phosphate G protein-coupled receptors. Faseb J. 2004;18(3):551–3.

172. EMA. Gilenya (fingolimod) [Internet]. 2011 [cited 2021 Jul 21]. Available from: https://www.ema.europa.eu/en/documents/overview/gilenya-epar-medicine-overview_en.pdf

173. Huwiler A, Zangemeister-Wittke U. The sphingosine 1-phosphate receptor modulator fingolimod as a therapeutic agent: Recent findings and new perspectives. Pharmacol Therapeut. 2018;185:34–49.

174. Scott LJ. Siponimod: A Review in Secondary Progressive Multiple Sclerosis. Cns Drugs. 2020;34(11):1191–200.

175. Martini S, Krämer S, Loof T, Wang-Rosenke Y, Daig U, Budde K, et al. S1P modulator FTY720 limits matrix expansion in acute anti-thy1 mesangioproliferative glomerulonephritis. Am J Physiol-renal. 2007;292(6):F1761–70.

176. Peters H, Martini S, Wang Y, Shimizu F, Kawachi H, Krämer S, et al. Selective lymphocyte inhibition by FTY720 slows the progressive course of chronic anti-thy 1 glomerulosclerosis. Kidney Int. 2004;66(4):1434–43.

177. Sui M, Zhou J, Xie R, Liu X, Mu S, Jia X, et al. The sphingosine-1-phosphate receptor agonist FTY720 prevents the development of anti-glomerular basement membrane glomerulonephritis. Mol Biol Rep. 2012;39(1):389–97.

178. Wolf AM, Eller K, Zeiser R, Dürr C, Gerlach UV, Sixt M, et al. The Sphingosine 1-Phosphate Receptor Agonist FTY720 Potently Inhibits Regulatory T Cell Proliferation In Vitro and In Vivo. J Immunol. 2009;183(6):3751–60.

179. Doorn R van, Pinheiro MAL, Kooij G, Lakeman K, Hof B van het, Pol SM van der, et al. Sphingosine 1-phosphate receptor 5 mediates the immune quiescence of the human brain endothelial barrier. J Neuroinflamm. 2012;9(1):133–133.

180. Jaillard C, Harrison S, Stankoff B, Aigrot MS, Calver AR, Duddy G, et al. Edg8/S1P5: An Oligodendroglial Receptor with Dual Function on Process Retraction and Cell Survival. J Neurosci. 2005;25(6):1459–69.

181. Walzer T, Chiossone L, Chaix J, Calver A, Carozzo C, Garrigue-Antar L, et al. Natural killer cell trafficking in vivo requires a dedicated sphingosine 1-phosphate receptor. Nat Immunol. 2007;8(12):1337–44.

182. Wünsche C, Koch A, Goldschmeding R, Schwalm S, Heringdorf DM zu, Huwiler A, et al. Transforming growth factor β2 (TGF-β2)-induced connective tissue growth factor (CTGF) expression requires sphingosine 1-phosphate receptor 5 (S1P5) in human mesangial cells. Biochimica Et Biophysica Acta Bba - Mol Cell Biology Lipids. 2015;1851(5):519–26.

183. Pardo AD, Castaldo S, Amico E, Pepe G, Marracino F, Capocci L, et al. Stimulation of S1PR5 with A-971432, a selective agonist, preserves blood–brain barrier integrity and exerts therapeutic effect in an animal model of Huntington's disease. Hum Mol Genet. 2018;27(14):2490–501.

184. Hundehege P, Cerina M, Eichler S, Thomas C, Herrmann A, Göbel K, et al. The next-generation sphingosine-1 receptor modulator BAF312 (siponimod) improves cortical network functionality in focal autoimmune encephalomyelitis. Neural Regen Res. 2019;14(11):1950.

185. Vogelgesang A, Domanska G, Ruhnau J, Dressel A, Kirsch M, Schulze J. Siponimod (BAF312) Treatment Reduces Brain Infiltration but Not Lesion Volume in Middle-Aged Mice in Experimental Stroke. Stroke. 2019;50(5):1224–31.

186. Carter D, He X, Munson S, Twigg P, Gernert K, Broom M, et al. Three-dimensional structure of human serum albumin. Science. 1989;244(4909):1195–8.

187. Birn H, Christensen EI. Renal albumin absorption in physiology and pathology. Kidney Int. 2006;69(3):440–9.

188. Larkins NG, Teixeira-Pinto A, Craig JC. A narrative review of proteinuria and albuminuria as clinical biomarkers in children. J Paediatr Child H. 2019;55(2):136–42.

189. Newman DJ, Pugia MJ, Lott JA, Wallace JF, Hiar AM. Urinary protein and albumin excretion corrected by creatinine and specific gravity. Clinica Chimica Acta. 1999;294:139–55.

190. Bakker AJ. Detection of microalbuminuria. Receiver operating characteristic curve analysis favors albumin-to-creatinine ratio over albumin concentration. Diabetes Care. 1999;22(2):307–13.

191. McManus JFA. The periodic acid routing applied to the kidney. Am J Pathol. 1948;24(3):643–53.

192. Malaprade L. Étude de l'action des polyalcools sur l'acide periodique et des periodates alcalins. Bulletin de la Société Chimique de France. 1934;1:833.

193. McManus JFA, Cason JE. Carbohydrate Histochemistry Studied By Acetylation Techniques. J Exp Medicine. 1950;91(6):651–4.

194. Ramos-Vara JA. Technical Aspects of Immunohistochemistry. Vet Pathol. 2005;42(4):405–26.

195. Engel P, Boumsell L, Balderas R, Bensussan A, Gattei V, Horejsi V, et al. CD Nomenclature 2015: Human Leukocyte Differentiation Antigen Workshops as a Driving Force in Immunology. J Immunol. 2015;195(10):4555–63.

196. Strobl H, Scheinecker C, Csmarits B, Majdic O, Knapp W. Flow cytometric analysis of intracellular CD6 8 molecule expression in normal and malignant haemopoiesis. Brit J Haematol. 1995;90(4):774–82.

197. Holness C, Simmons D. Molecular cloning of CD68, a human macrophage marker related to lysosomal glycoproteins. Blood. 1993;81(6):1607–13.

198. Kurushima H, Ramprasad M, Kondratenko N, Foster DM, Quehenberger O, Steinberg D. Surface expression and rapid internalization of macrosialin (mouse CD68) on elicited mouse peritoneal macrophages. J Leukocyte Biol. 2000;67(1):104–8.

199. Rock KL, Reiser H, Bamezai A, Mcgrew J, Benacerraf B. The LY-6 Locus: A Multigene Family Encoding Phosphatidylinositol-Anchored Membrane Proteins Concerned with T-Cell Activation. Immunol Rev. 1989;111(1):195–224.

200. Lee PY, Wang J, Parisini E, Dascher CC, Nigrovic PA. Ly6 family proteins in neutrophil biology. J Leukocyte Biol. 2013;94(4):585–94.

201. DF S. Neutrophil-specific antigen HNA-2a, NB1 glycoprotein, and CD177. Current Opinion in Hematology. 2017;14(6):688–93.

202. M GN. Avidin. 1. The Use Of [14C]Biotin For Kinetic Studies And For Assay. Biochem J. 1963;89(3):585–91.

203. Eakin RE, McKinley WA, Williams RJ. Egg-White Injury In Chicks And Its Relationship Ta A Deficiency Of Vitamin H (Biotin). Science. 1940;92(2384):224–5.

204. Bratthauer GL. Immunocytochemical Methods and Protocols. Methods Mol Biology. 2009;588:257–70.

205. Liu Y, Goff RD, Zhou D, Mattner J, Sullivan BA, Khurana A, et al. A modified α-galactosyl ceramide for staining and stimulating natural killer T cells. J Immunol Methods. 2006;312(1–2):34–9.

206. Hobson AD, Harris CM, Kam EL van der, Turner SC, Abibi A, Aguirre AL, et al. Discovery of A-971432, An Orally Bioavailable Selective Sphingosine-1-Phosphate Receptor 5 (S1P5) Agonist for the Potential Treatment of Neurodegenerative Disorders. J Med Chem. 2015;58(23):9154–70.

207. Blanchard O, Stepanovska B, Starck M, Erhardt M, Römer I, Heringdorf DM zu, et al. Downregulation of the S1P Transporter Spinster Homology Protein 2 (Spns2) Exerts an Anti-Fibrotic and Anti-Inflammatory Effect in Human Renal Proximal Tubular Epithelial Cells. Int J Mol Sci. 2018;19(5):1498.

208. Xu M, Liu D, Ding L hong, Ma K ling, Wu M, Lv L li, et al. FTY720 inhibits tubulointerstitial inflammation in albumin overload-induced nephropathy of rats via the Sphk1 pathway. Acta Pharmacol Sin. 2014;35(12):1537–45.

209. Wang X, Yu Y, Li M, Yu Y, Liu G, Xie Y, et al. Sphingosine 1-phosphate alleviates Coxsackievirus B3-induced myocarditis by increasing invariant natural killer T cells. Exp Mol Pathol. 2017;103(2):210–7.

210. Ferraro D, Biasi SD, Simone AM, Orlandi R, Nasi M, Vitetta F, et al. Modulation of Tregs and iNKT by Fingolimod in Multiple Sclerosis Patients. Cells. 2021;10(12):3324.

211. Aubin JE. Autofluorescence of viable cultured mammalian cells. J Histochem Cytochem Official J Histochem Soc. 1979;27(1):36–43.